

Research

**Review and Assessment of SCC Experiments
with RPV Steels in Oskarshamn 2 and 3
(ABB Report SBR 99-020)**

Hans-Peter Seifert
Stefan Ritter

November 2005

SKI perspective

Background

Some years ago SKI and the Swedish utilities sponsored a project following some alarming results concerning stress corrosion crack growth rates in reactor pressure vessel steels in simulated BWR environments, which were published in the late eighties and early nineties. The aim of this project was to investigate the relevance of these results for Swedish reactor pressure vessels.

In the Swedish project, the susceptibility of reactor pressure vessel steels to stress corrosion cracking was investigated in BWR environments for up to five years and the results were reported by ABB Atom AB. The project comprised a large number of bolt-loaded pressure vessel steel samples including some clad with typical weld metal (Inconel 182) and some with side plates to aggravate the conditions for stress corrosion cracking. In one of the Inconel 182 clad specimens marked crack growth was observed in the pressure vessel steel. In this case the pre-fatigue crack tip was located in the reactor pressure vessel steel base metal beyond its heat-affected zone. This was an unexpected and exceptional result, so further fractographic and metallographic investigations were performed by VTT in an attempt to clarify the reasons for this unique observation.

The cracking in this specific specimen was found to be due to stress corrosion cracking in the reactor pressure vessel steel that could not be related to any mistreatment of the specimen, welding defects, testing artefacts or microstructural anomalies. Thus no completely satisfactory explanation for this unexpected result could be forwarded and it was deemed necessary to initiate further work to try and put these results in perspective. Hans-Peter Seifert and Stefan Ritter, PSI, are leading experts in this field and were therefore engaged for this additional work.

Purpose of the project

In an attempt to explain the reason for the unexpected crack growth in one of the specimens clad with Inconel 182, PSI was asked to prepare a state-of-the-art report on environmentally-assisted cracking of low-alloy reactor pressure vessel steels (see SKI 2005:60), and to critically review and reassess the Swedish work in this area. These two documents are intended to support SKI with decision making as to whether or not there is a substantial risk for stress or strain-induced corrosion cracking in Swedish nuclear reactor pressure vessels, if for example a crack propagates through the cladding or an attachment weld to the underlying low alloy steel.

Results

Although the extent of cracking was rather surprising for a bolt-loaded specimen, the average stress corrosion crack growth rate of 0.5 mm/year over the five-year testing period does not represent an immediate concern. The overwhelming part of crack growth can have occurred during a 20 day chloride transient during the third year of exposure because of a condenser leakage after an outage. The test results fit well to the experimental background knowledge and have basically confirmed the excellent service record of properly fabricated carbon and low alloy steel primary pressure-boundary components, where to date, no cases of stress corrosion cracking have been observed .

There is therefore a limited risk that an interdendritic stress corrosion crack in the Inconel 182 weld metal of an attachment weld or in regions with Inconel 182 cladding might propagate to the adjacent reactor pressure vessel steel. Even in this rare case, only very limited stress corrosion cracking or strain induced stress corrosion cracking in the thick-walled reactor pressure vessel is expected as long as prolonged and severe chloride excursions are avoided and the number of plant transients is limited.

Although there is no direct evidence from the field of stress corrosion cracking risks in reactor pressure vessels, the effect of chloride excursions on stress corrosion cracking crack growth in reactor pressure vessel steels under BWR normal water chemistry conditions, and in particular the possibility of long-term effects after severe and prolonged transients, should, in the opinion of PSI be evaluated further.

Effects on SKI work

The conclusions below are drawn using both this study and the study presented in SKI 2005:60 and are valid for both.

Both studies are a step towards understanding the behaviour of carbon and low-alloy steels in the environment prevailing in nuclear power plants. Understanding the underlying cause of environmentally assisted cracking is necessary, to be able to have an effective inspection program and mitigate it if necessary.

Though the overwhelming part of the crack growth seems to have occurred during a chloride transient and laboratory experience presented in SKI 2005:60, clearly demonstrate that chloride transients have an increasing effect on stress corrosion crack growth rate in carbon and low alloy steels, the explanation given by PSI that a chloride transient is the cause of excessive crack growth rate appears reasonable.

Even in such cases only very limited stress corrosion cracking or strain induced stress corrosion cracking is expected as long as prolonged and severe chloride excursions are avoided and the number of transients are limited.

Prolonged, severe or numerous chloride transients are not expected to occur in nuclear power plants operating under normal conditions. In addition the pressure vessel steels used in Swedish nuclear power plants have a low sulphurous content which has also been shown to be favourable with regard to stress corrosion cracking. The risk of excessive crack growth in pressure vessel steels in Swedish nuclear power plants, due to stress corrosion cracking or strain induced corrosion cracking is therefore estimated to be low.

Although it is of scientific interest to investigate the effect of chloride excursions on stress corrosion cracking crack growth rate in reactor pressure vessel steels under BWR normal water chemistry conditions, and in particular the possibility of long-term effects after severe and prolonged transients, SKI currently consider that there is no need for further work considering the conditions which have been demonstrated to prevail in Swedish nuclear power plants.

Project information

Behnaz Aghili has been responsible for the project at SKI.
SKI reference: SKI 2005/309/200341002.

Research

Review and Assessment of SCC Experiments with RPV Steels in Oskarshamn 2 and 3 (ABB Report SBR 99-020)

Hans-Peter Seifert
Stefan Ritter

Paul Scherrer Institute
Laboratory for Materials Behaviour
Nuclear Energy and Safety Research Department
5232 Villigen PSI
SWITZERLAND
E-Mail: hans-peter.seifert@psi.ch

November 2005

This report concerns a study which has been conducted for the Swedish Nuclear Power Inspectorate (SKI). The conclusions and viewpoints presented in the report are those of the author/authors and do not necessarily coincide with those of the SKI.

Executive Summary

Some years ago SKI and the Swedish utilities sponsored SCC investigations, where non-cladded and cladded (Inconel 182/AISI 308L) bolt-loaded C(T) specimens of different reactor pressure vessel (RPV) steels have been exposed to boiling water reactor (BWR)/normal water chemistry (NWC) and hydrogen water chemistry (HWC) environment in Oskarshamn 3 and 2 during a five- and four-year period. In the following report, the Swedish stress corrosion cracking (SCC) data from this project are critically reviewed and assessed on the basis of the relevant service experience and of the accumulated experimental background knowledge on SCC of carbon (C) and low-alloy steel (LAS) and dissimilar weld joints in high-temperature (HT) water.

The investigations in Oskarshamn 3/2 generally revealed a low SCC crack growth susceptibility of RPV steels and interdendritic (ID) SCC in the Inconel 182 weld metal under BWR/NWC and HWC conditions. All non-cladded specimens and specimens with AISI 308L stainless steel cladding revealed no or only minor crack growth under both BWR/NWC and HWC conditions. However, the specimens with Inconel 182 cladding and fatigue pre-crack in the weld metal revealed clear, but minor crack growth into the heat-affected zone (HAZ) of the RPV steel under BWR/NWC conditions. Marked crack growth (of 2.43 mm) in the RPV steel was only observed in one of the Inconel 182 cladded specimens tested under BWR/NWC conditions with a high K_I value of 48.8 MPa·m^{1/2}, where the fatigue pre-crack-tip was located in the RPV steel base metal far beyond its HAZ. Detailed post-test fracto- and metallography confirmed that cracking in this specimen was due to SCC and it could be neither related to any mistreatment of specimen, welding defects, testing artefacts nor to any microstructural anomalies.

Although the extent of cracking was rather surprising for a bolt-loaded specimen, the average SCC crack growth rate (CGR) of 0.5 mm/year over the five-year testing period was still within the upper range of constant load SCC CGRs in autoclave tests in oxygenated high-purity water and below the BWRVIP-60 SCC disposition line (DL) 1, and thus does not represent an immediate concern. The initial K_I value of this specimen represents a rather deep crack in the RPV and was close to the K_I range of 50 to 70 MPa·m^{1/2}, where accelerated SCC is usually observed in high-purity water, in particular in high-sulphur steels. Based on recent lab experiments at PSI with chloride excursions, an alternate explanation for the cracking in this specimen could be given: The overwhelming part of crack growth might also have occurred during a 20 day chloride transient of 5 to 30 ppb, which happened during the third year of exposure because of a condenser leakage briefly after an outage, where some crack-tip straining or local SCC/SICC crack growth might still have been present. This was also further confirmed by the DCPD measurements during the shut-down periods, which indicated that more than 80 % of crack growth had occurred during the third year of exposure.

The test results fit well to the experimental background knowledge and have basically confirmed the excellent service record of properly fabricated C & LAS primary pressure-boundary components, where no cases of SCC were observed so far. The specimens with the susceptible Inconel 182 cladding and fatigue pre-crack in the weld metal revealed clear, but minor crack growth into the HAZ of the RPV steel under BWR/NWC conditions. They thus confirm the possibility of SCC crack growth through the fusion line into the adjacent RPV steel. Although in the field the cracking in dissimilar welds was usually confined to the weld metal and some lab experiments revealed cessation of SCC at the fusion boundary. Based on the test data in Oskarshamn 3 and lab experience, the possibility of slow SCC crack growth with CGRs < 0.6 mm/year at K_I values < 60 MPa·m^{1/2} in the unaffected RPV base metal cannot be fully excluded. There is thus a certain risk that an ID SCC crack in the Inconel 182 weld metal of an attachment weld or in regions with Inconel 182 cladding might propagate to

the adjacent RPV steel. Even in this rare case, only very limited SCC/SICC cracking in the thick-walled RPV is expected as long as prolonged and severe chloride excursions are avoided and the number of plant transients is limited.

It is therefore recommended to perform careful flaw tolerance evaluations (e.g., based on the BWRVIP-60 SCC DLs and the Code Case N-643 EAC curve) for different relevant Inconel 182 weld configurations with initial cracks, which slightly reach into the RPV steel, to estimate the effective margins with respect to current intervals of the periodic in-service inspection. If margins are sufficiently high, no further immediate actions are necessary. The reliable measurement/modelling of the residual stress profiles in such attachment welds may be essential to avoid any undue conservatism in such structural integrity assessments.

Whether or not an ID SCC crack in the weld metal may cross the fusion line and enter into the adjacent RPV steel can strongly depend on the main dendrite orientation (solidification structure), the distribution of grain boundary misorientation in the weld, the plastic weld shrinkage strain and residual stress levels/profiles with respect to the RPV, as well as on the extent of dilution between weld and base metal or possibility of susceptible microstructures/excessive hardness in the weld HAZ, etc. Thus analysis of weld metallurgy/residual stress profiles of relevant Inconel 182 attachment welds and claddings could eventually help to identify regions with the highest risk.

If further reactor site testing is considered, the authors would place the focus on tests under BWR/NWC conditions with Inconel 182-RPV weld joints (representative for relevant Swedish configurations) with fatigue pre-crack-tips close to the fusion line and realistic initial K_I values to study the crack extension to the RPV over prolonged periods. Tests with specimens with crack planes parallel to fusion boundary or weld configurations with more favourable dendrite orientations or Inconel 82 weldments could complete the testing programme. If possible, some specimens should also be tested in lab experiments under comparable environmental conditions and active external loading with continuous online crack length measurements by DCPD.

Although there is no direct evidence from the field, with respect to SCC risks in RPVs, the effect of chloride excursions on SCC crack growth in RPV steels under BWR/NWC conditions, and in particular the possibility of long-term effects after severe and prolonged transients, should be further evaluated. Long-term tests with bolt-loaded specimens and moderate chloride contents of 5 to 20 ppb could complete such a testing programme. Studies on the possible interaction between chloride and oxide films/repassivation in HT water could help to better understand the effect of chlorides on the SCC behaviour.

Table of Contents

0 LIST OF ABBREVIATIONS.....	5
1 INTRODUCTION.....	7
1.1 BACKGROUND AND GOALS OF THE REPORT.....	7
1.2 STRUCTURE OF THE REPORT.....	7
2 SUMMARY OF THE SCC EXPERIMENTS WITH RPV STEELS IN OSKARSHAMN 3/2 ..	8
2.1 MATERIALS, TEST PROCEDURE, FACILITIES AND CONDITIONS	8
2.2 MAJOR TEST RESULTS	10
3 SUMMARY OF RELEVANT SERVICE EXPERIENCE AND EXPERIMENTAL KNOWLEDGE.....	11
3.1 SCC OF C & LAS IN HIGH-TEMPERATURE WATER	11
3.1.1 <i>Service Experience</i>	11
3.1.2 <i>SCC Susceptibility Conditions</i>	11
3.1.3 <i>SCC Crack Growth</i>	11
3.1.4 <i>SCC Crack Growth During and After Chloride Excursions</i>	15
3.2 SCC IN DISSIMILAR WELD JOINTS	19
3.2.1 <i>Service Experience</i>	19
3.2.2 <i>SCC in Inconel 182 Dissimilar Weld Metals</i>	20
4 EVALUATION AND ASSESSMENT OF THE SCC DATA FROM OSKARSHAMN 2/3	28
4.1 RELEVANCE OF TEST MATERIALS, PROCEDURES AND CONDITIONS.....	28
4.1.1 <i>Materials</i>	28
4.1.2 <i>Applied Test Procedure</i>	28
4.1.3 <i>Test Conditions</i>	28
4.2 EVALUATION AND ASSESSMENT OF THE TEST RESULTS.....	29
4.3 ASSESSMENT AND POSSIBLE EXPLANATION FOR SCC IN SPECIMEN 402	34
5 SUMMARY AND CONCLUSIONS	39
6 RECOMMENDATIONS.....	40
7 ACKNOWLEDGEMENTS.....	41
8 REFERENCES.....	42

0 List of Abbreviations

Abbreviations:

ABB	Asea Brown Boveri
ASME BPV	ASME Boiler and Pressure Vessel Code
ASTM E 399	Test method for plane-strain fracture toughness of metallic materials
BWR	Boiling water reactor
BWRVIP	Boiling Water Reactor Vessel and Internals Project
C & LAS	Carbon and low-alloy steel
C(T)	Compact tension (specimen)
CGR	Crack growth rate
COD	Crack opening displacement
DCPD	Direct current potential drop (method)
DL	Disposition line
DO	Dissolved oxygen
DSA	Dynamic strain ageing
EAC	Environmentally-assisted cracking
ECP	Electrochemical corrosion potential
EPRI	Electric Power Research Institute
GE	General Electric
HAZ	Heat-affected zone
HWC	Hydrogen water chemistry
ID	Interdendritic
IG	Intergranular
LWR	Light water reactor
MPA	Staatliche Materialprüfungsanstalt, University of Stuttgart, Germany
NWC	Normal water chemistry
PPU	Periodical partial unloading
PSI	Paul Scherrer Institute, Villigen, Switzerland
PWHT	Post-weld heat treatment
PWR	Pressurized water reactor
RPV	Reactor pressure vessel
SCC	Stress corrosion cracking
SEM	Scanning electron microscope
SHE	Standard-hydrogen electrode
SICC	Strain-induced corrosion cracking
SKI	Swedish Nuclear Power Inspectorate, Stockholm, Sweden
TG	Transgranular
VTT	Technical Research Centre of Finland, Espoo, Finland
WOL	Wedge-opening loaded (specimens)

Symbols and Units:

Symbol	Unit	Designations
Δa_{EAC}	μm or mm	Crack advance (by EAC)
a	mm	Crack length
$\Delta a/\Delta N$	$\mu\text{m}/\text{cycle}$	Crack advance per fatigue cycle
da/dt	m/s	Time-based crack growth rate: time-derivate of $a(t)$
da/dt_{SCC}	m/s	Time-based SCC crack growth rate in high-temperature water
DO	ppb or ppm	Concentration of dissolved oxygen
COD	μm	Crack opening displacement
$d\epsilon/dt$	s^{-1}	Strain rate
$d\epsilon_{CT}/dt$	s^{-1}	Crack-tip strain rate
dK_I/dt	$\text{MPa}\cdot\text{m}^{1/2}/\text{h}$	Stress intensity factor rate
ΔK	$\text{MPa}\cdot\text{m}^{1/2}$	$\Delta K = K_I^{\text{max}} - K_I^{\text{min}}$: Total stress intensity factor range
ECP	mV_{SHE}	Electrochemical corrosion potential
ν	Hz	Frequency
κ	$\mu\text{S}/\text{cm}$	Specific electric conductivity
K_I	$\text{MPa}\cdot\text{m}^{1/2}$	Stress intensity factor
$K_{I,ASTM}$	$\text{MPa}\cdot\text{m}^{1/2}$	ASTM E 399 limit for K_I
K_{IJ}	$\text{MPa}\cdot\text{m}^{1/2}$	K_I value at the onset of ductile crack growth in inert environment
N	–	Cycle number
R	–	Load-ratio: $R = P_{\text{min}} / P_{\text{max}}$
T	$^{\circ}\text{C}$	Temperature

1 Introduction

1.1 Background and Goals of the Report

Some years ago SKI and the Swedish utilities sponsored a project following the alarming results on stress corrosion crack growth rates (CGRs) in reactor pressure vessel (RPV) steels, which were published in the late eighties and early nineties [1]. The aim of this project was to demonstrate that the risk for stress corrosion cracking (SCC) in the Swedish RPVs is minimal.

Within this project, the susceptibility of RPV steels to SCC has been investigated in realistic BWR environment and the results have been reported by ABB in the Report SBR 99-020 [2]. For this reason bolt loaded modified C(T) specimens of different RPV steels were exposed to BWR/normal water chemistry (NWC) environment during a five-year period in Oskarshamn 3, and to BWR/hydrogen water chemistry (HWC) environment during a four-year period in Oskarshamn 2. In total 72 C(T) specimens (36 in BWR/NWC and 36 in BWR/HWC) were tested at different stress intensity levels. Twelve C(T) specimens were multipass clad with either Inconel 182 or stainless steel AISI 308L and post-weld heat treated at 620 °C for 8 h to simulate cladding or attachment welds.

All non-clad specimens and specimens with 308L stainless steel cladding revealed no or only minor crack growth under both BWR/NWC and HWC conditions. However, some of the clad specimens tested in BWR/NWC environment revealed clear, but minor crack growth into the HAZ of the RPV steel. Marked crack growth of 2.43 mm in the pressure vessel steel was only observed in one of the Inconel 182 clad specimens, where the pre-fatigue crack tip was located in the RPV steel base metal beyond its heat-affected zone (HAZ) (specimen 402). Due to this unexpected result, further fractographic and metallographic investigations have been performed by VTT on five of the 72 C(T) specimens in order to clarify the reasons for this unexpected cracking [3].

The cracking in C(T) specimen 402 was found to be due to SCC in the RPV steel and could not be related to any mistreatment of specimen/welding defects, testing artefacts or microstructural anomalies and no completely satisfactory explanation for this unexpected result could be forwarded. PSI was therefore asked by SKI to prepare a state-of-the-art report on EAC of low-alloy RPV steels [4] and to critically review and reassess the Swedish work in this area in a second report. These two documents shall support SKI with decision making as whether or not there is a substantial risk for stress or strain-induced corrosion cracking in Swedish nuclear RPVs, if for example a crack in the cladding or an attachment weld propagates to the underlying LAS.

1.2 Structure of the Report

In the present report, the Swedish SCC test data on low-alloy RPV steels in Oskarshamn 2 and 3 are critically reviewed and assessed on the basis of the state-of-the-art report on EAC of low-alloy RPV steels [4] and on the PSI testing experience in this field. In Section 2, the Swedish reactor site test data as well as the main results of the fractographical evaluations at VTT are summarized in a condensed form. In Section 3 the most relevant aspects of service experience and experimental background knowledge on SCC in C & LAS and in Inconel 182/LAS dissimilar welds are briefly discussed as far as it is required for the evaluation and assessment of the Swedish EAC test data in Section 4. Based on the summary of the main results and conclusions of this critical assessment in Section 5, some few recommendations are worked out in Section 6.

2 Summary of the SCC Experiments with RPV Steels in Oskarshamn 3/2

2.1 Materials, Test Procedure, Facilities and Conditions

Fatigue pre-cracked bolt loaded modified 25 mm thick compact tension C(T) specimens (Figure 1) of three different RPV steels with sulphur contents of 0.012 to 0.016 wt.% S (Table 1) were exposed to BWR/NWC environment during a five-year period in a test loop in Oskarshamn 3, and to BWR/HWC environment during a four-year period in a filter vessel in Oskarshamn 2. In both loops specimens were exposed to primary recirculation water of full temperature of approximately 270 to 275 °C. The test loop in Oskarshamn 3 is connected at the pressure side of reactor water clean-up system (RWCU) pumps. The filter vessels in Oskarshamn 2 are located in a large by-pass flow at the full temperature influent of the RWCU system. In both loops, non-turbulent, but flowing conditions prevailed at the specimens surfaces.

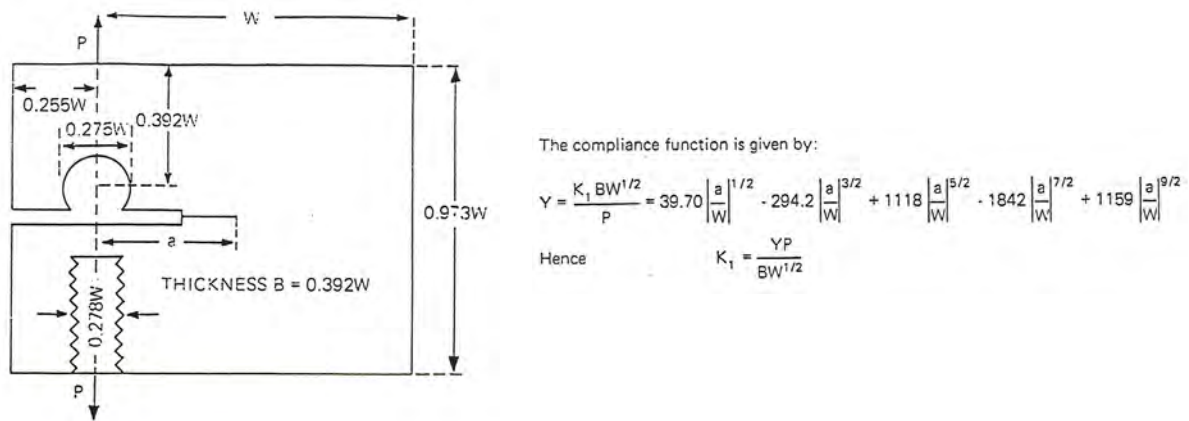


Figure 1: Schematic of bolt-loaded modified C(T) specimen with formula for K_I calculation.

Material	C	Si	Mn	P	S	Cr	Ni	Mo	Co	V	Cu	Ti	Al	Slag group/ no.
A533B Cl. 1 EPRI 1b H		0.25	1.32	0.012	0.016	0.075	0.63	0.55	<0.1	<0.01	0.1	<0.01	0.029	A, thin/ 1.5
A533B Cl. 1 55057-1	0.165 0.175	0.22	1.38	0.01	0.013	0.093	0.55	0.53	0.014	<0.01	0.1	<0.01	0.017	A, thin/ 1.0
A508 Cl.3 45K1868	0.2	0.27	0.67	0.012	0.012	0.38	0.80	0.65	0.012	<0.01	0.13	<0.01	0.022	A, thin/ 1.0

Table 1: Chemical composition of investigated RPV steels in wt.% (check analysis).

During the five-year NWC exposure period in Oskarshamn 3, the conductivity and the dissolved oxygen content in the reactor water varied between 0.08 and 0.13 $\mu\text{S}/\text{cm}$ and 250 to 370 ppb and were mostly below 0.09 $\mu\text{S}/\text{cm}$ and between 300 and 350 ppb. Apart from SiO_2 (typically 200 to 400 ppb, up to 577 ppb), the impurity content (typically < 1 ppb Cl^- , 1 to 2 ppb SO_4^{2-}) was very low for the overwhelming part of the operation period and with one exception only few minor short-term excursions occurred. During the third year of operation, there was a significant chloride transient of 5 to 30 ppb during a period of three weeks because of a condenser leakage briefly after an outage.

During the four-year HWC exposure period in Oskarshamn 2, the HWC availability (with ECP of stainless steel piping < -230 mV_{SHE}) varied between 77 and 94 %. During the HWC periods the dissolved oxygen concentration was < 1 ppb and conductivity $\leq 0.06 \mu\text{S}/\text{cm}$ and ECP of 304 stainless steel RWCU pipe was between -500 and -300 mV_{SHE} . Short conductivity transients of 1 to 2 days were usually observed when the reactor went off HWC, before low

conductivities $< 0.1 \mu\text{S}/\text{cm}$ were re-established. These conductivity transients were caused by chromate due to changes in oxide films. During NWC periods, the dissolved oxygen content was typically between 200 to 400 ppb and ECP temporarily reached high values of 0 to $+100 \text{ mV}_{\text{SHE}}$. Apart from the mentioned temporary CrO_4^{2-} -peaks and SiO_2 (typically 200 to 400 ppb, up to 685 ppb), the impurity content (typically $< 1 \text{ ppb Cl}^-$, 1 to 4 ppb SO_4^{2-}) was very low during the whole part of the operation period.

In total 72 C(T) specimens (36 in BWR/NWC and 36 in BWR/HWC) were tested at stress intensity levels between 17.2 and $54.6 \text{ MPa}\cdot\text{m}^{1/2}$. The RPV steel specimens were oriented in the T-S direction, thus the crack front was parallel to the rolling/main working direction. Twelve C(T) specimens were multipass cladded with either Inconel 182 or stainless steel AISI 308L and post-weld heat treated at $620 \text{ }^\circ\text{C}$ for 8 h to simulate cladding or attachment welds. For this reason, an U-shaped groove in the RPV steel specimen blanks was filled by multipass shielded metal arc welding (SMAW) with Inconel 182 or stainless steel AISI 308L (Table 2 and Figure 2). The welding interpass temperature was $< 100 \text{ }^\circ\text{C}$ to avoid unrealistic weld sensitization during welding. The pre-fatigue crack were located either in the pressure vessel (in 4 specimens with Inconel 182 and AISI 308L weld metal) or in the weld metal (in 4 specimens with Inconel 182 cladding). In the later case, the pre-cracks were parallel to the main weld dendrites. After welding the specimens were post-weld heat treated for 8 h at $620 \text{ }^\circ\text{C}$, followed by furnace cooling with $10 \text{ }^\circ\text{C}/\text{h}$ to $200 \text{ }^\circ\text{C}$.

Material	C	Si	Mn	P	S	Cr	Ni	Mo	Co	V	Cu	Ti	Al	Nb	Fe
A533B Cl. 1	0.165 0.175	0.22	1.38	0.01	0.013	0.093	0.55	0.53	0.014	<0.01	0.1	<0.1	0.017		bal.
Inconel 182	0.041	0.49	7.4	<0.005	<0.005	14.2	bal.	<0.05	0.04	–	0.02	0.45	0.052	1.6	8
AISI 308L	0.025	0.87	0.79	0.018	0.008	18.7	10.2	0.1	0.03	0.07	0.05	<0.1	<0.1	<1	bal.

Table 2: Chemical composition of cladded RPV and austenitic cladding materials in wt.%.

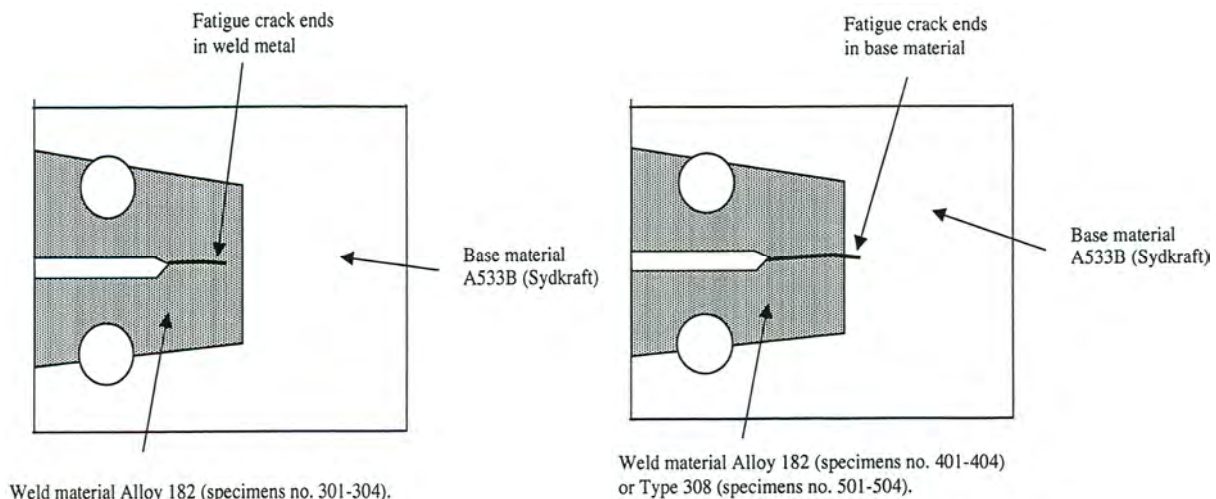


Figure 2: Schematic of RPV specimens with Inconel 182 and AISI 308L cladding.

After pre-cracking to a specific initial crack length, the specimens were loaded to a specified K_I value at room temperature in an Instron tensile testing machine with simultaneous measurement of the crack-opening displacement (COD). The required bolt load P was calculated using the expression published by Walker and May [5], see Figure 1. The machine load was then decreased stepwise, 5 %, and the bolt was fastened carefully until the intended COD reading was reached. This procedure was repeated until the bolt was carrying the full load. The bolts were made from the high strength LAS Cr-Ni-Mo-steel SS 2541 for the RPV steels specimens and the high-strength Ni-base alloy X-750 for the cladded specimens.

The crack length was measured intermittently by the direct current potential drop method (DCPD) during the annual revisions and before the specimens were exposed to the test environment. All specimens were ultrasonically cleaned before DCPD measurements. The accuracy of the DCPD system and applied procedure was such that it would detect an average crack length beyond the notch of 0.1 to 0.2 mm in the Inconel 182 weld metal and of 0.3 to 0.5 mm in the RPV steels.

After completion of testing the specimens were decontaminated electrochemically in a solution of oxalic and citric acid using a small current. Thereafter, the specimens were fatigued for a certain distance at room temperature and then broken open in an Instron tensile testing machine. Fractographic examination of all test specimens was performed to obtain information on crack growth. The average initial and final crack length and the position of the initial and final crack with respect to the fusion line in case of clad specimens was calculated from 25 equidistant measurements along the crack front.

2.2 Major Test Results

The tests basically revealed a very low SCC crack growth susceptibility of RPV steels under representative BWR/NWC and HWC conditions. All non-clad specimens and specimens with stainless steel 308L cladding revealed no or only very minor (< 0.24 mm) crack growth in both NWC and HWC environments, which usually appeared as a ditch on the fracture surfaces, probably from general corrosion.

In specimens with Inconel 182 claddings and fatigue pre-crack tips in the weld metal, interdendritic (ID) SCC was observed in the weld metal in both NWC and HWC environments. Under NWC conditions, the cracks further propagated to the LAS HAZ to a remarkable but limited extent, whereas under HWC conditions significantly smaller crack extension had occurred and the crack fronts were therefore still in the weld metal far away from the fusion line. In the specimens tested under NWC conditions, also some crack extension along the fusion line was also observed locally in regions with martensitic or carbide-rich microstructure and very high microhardness of up to 500 HV0.05.

In specimens with Inconel 182 cladding and fatigue pre-crack tips in the LAS base metal, only minor crack growth was observed under HWC conditions (0.06 mm) and in one of the two specimens under NWC conditions with the lower applied stress intensity factor (0.14 mm). However, marked crack growth of 2.43 mm in the pressure vessel steel was observed in the second Inconel 182 clad specimens, where the pre-fatigue crack tip was located in the pressure vessel steel base metal beyond its HAZ (specimen 402).

Due to this unexpected result, further fractographic and metallographic investigations have been performed by VTT on five of the 72 modified compact C(T) specimens in order to clarify the reasons for this unexpected cracking and the results of these investigations were presented in a VTT report [3].

The cracking in the C(T) specimen 402 was found to be due to SCC in the RPV steel and could not be related to any mistreatment of specimen/welding defects, testing artefacts or microstructural anomalies. Although the area fraction of inclusions was high, within the range reported in literature for materials with increased EAC susceptibility due to MnS-inclusions, no completely satisfactory explanation for this unexpected result could be forwarded.

3 Summary of Relevant Service Experience and Experimental Knowledge

3.1 SCC of C & LAS in High-Temperature Water

3.1.1 Service Experience

The accumulated operating experience and performance of C & LAS primary pressure-boundary components in BWR and PWR is very good worldwide. However, isolated instances of EAC have occurred, particularly in BWR service, most often in LAS piping and, very rarely, in the RPV itself [4]. Oxidizing agents, usually dissolved oxygen, and relevant dynamic straining due to thermal stratification/stripping (e.g., during hot stand-by at low feedwater flow rate), or due to thermal and pressurisation cycles (e.g., plant-start-up/shut-down, hot stand-by, turbine rolls, etc.) were always involved. These cases were attributed either to strain-induced corrosion cracking (SICC) or corrosion fatigue [4]. Cracking incidents with a major, or even relevant, contribution of SCC to the total crack advance in properly manufactured and heat-treated C & LAS primary pressure-boundary components have not been reported. [4]

3.1.2 SCC Susceptibility Conditions

SCC initiation from smooth, defect-free surfaces under static load is generally only observed for stresses at the water-wetted surface above the high-temperature (HT) yield stress, quasi-stagnant flow conditions and increased concentration levels of anionic impurities such as SO_4^{2-} or Cl^- . If complete exhaustion of low-temperature creep was allowed to occur before the specimens were exposed to high-purity, HT water, no SCC was observed, thus indicating non-classical SCC behaviour and confirming the importance of dynamic straining for EAC of LAS in HT water. [4]

3.1.3 SCC Crack Growth

SCC in Passively Loaded (Wedge- or Bolt-Loaded) Specimens: In old investigations at ETH [1], usually 5 to 20 % of the tested WOL specimens have shown fast SCC with very high SCC CGRs of up to $5 \cdot 10^{-8}$ m/s down to low stress intensity factors of $20 \text{ MPa} \cdot \text{m}^{1/2}$ in static autoclave tests. These high SCC CGRs were mainly related to aggressive, poorly controlled environmental conditions (increased chloride and sulphate levels ≥ 100 ppb, $0.3 \mu\text{S}/\text{cm}$ (start of test) $\rightarrow 5$ to $10 \mu\text{S}/\text{cm}$ (end of the test)), which are not representative for current LWR power operation and/or to mechanical loading conditions with severe violation of small scale yielding conditions, which are not transferable to thick-walled components. [4]

Occurrence of SCC in constant-displacement tests with WOL specimens in modern HT water loops at PSI had been reported prior to 1993 [6]. In these tests, only a small proportion (5 to 20 %) of each set of specimens tested under nominally identical conditions revealed fast SCC. Loading of these specimens was done by pressing an Alloy 718 wedge to the notch of the DCB specimens in a hydraulic hand press and the measurement of COD at specimen front face with a rather simple device. Interestingly, some specimens tested at low, nominal K_I values revealed significant macro-branching of the crack path, which was also inclined at ca. 45° with respect to the specimen mid-plane. Fractographic inspection by scanning electron microscope (SEM) revealed significant amounts of ductility (dimple structure on the fracture surface) at the pre-crack front and near to the specimen surface [7], which may be regarded as a clear evidence for some relevant overloading of these specimens and significantly higher applied K_I values than indicated. Corrosion-assisted cracking had been reported for tests in oxygenated hot water with $\text{DO} > 200$ ppb and $K_I > K_{I,ASTM}$ for $\kappa = 1 \mu\text{S}/\text{cm}$, or $K_I > 2 \cdot K_{I,ASTM}$ for $\kappa = 0.5 \mu\text{S}/\text{cm}$. Additionally, it was stated that SCC had only been observed in those cases

where the specimens had been re-used in several tests, with either an increase of load, or with the introduction of a new fatigue pre-crack before the final phase of the experiment. In a subsequent project it has been demonstrated, that this kind of load increase is very questionable and difficult to control. On the basis of the original results, it was suggested that the initiation of SCC in WOL tests may be a statistical problem [1].

Following this statistical argument, a large number of WOL-DCB specimens (> 250 specimens) were tested in a subsequent project (1996 – 1998) [7]. Compared to the old project, the quality of the experimental work, in particular monitoring and evaluation of the data, was improved significantly. The loading was done very carefully in an electromechanical tensile machine with special loading frame for pressing the Alloy 718 wedge to the notch of DCB specimens with on-line monitoring of load and COD at the front face with a sophisticated and very accurate measurement device. During this project, no SCC could be initiated in the same materials in chloride-free, oxygenated HT water (up to 8 ppm DO and 370 ppb SO_4^{2-}) for testing periods up to 3000 h (Figure 3). From a total of > 250 individual specimens tested under constant displacement, just one specimen revealed a minor fractographic irregularity, and this was limited to the vicinity of a large MnS stringer. This specimen was tested at $1 \mu\text{S}/\text{cm}$ ($360 \text{ ppb } \text{SO}_4^{2-} > \text{EPRI action level 3}$), high ECP (8 ppm DO content), and at a high K_I value of $96 \text{ MPa}\cdot\text{m}^{1/2}$ ($K_I > 2 K_{I,ASTM}$). In the subsequent fractographic analysis by SEM, no conclusive evidence for corrosion-assisted cracking could be found. MPA Stuttgart has also observed no SCC in similar tests with 10 mm thick WOL-DCB specimens [8].

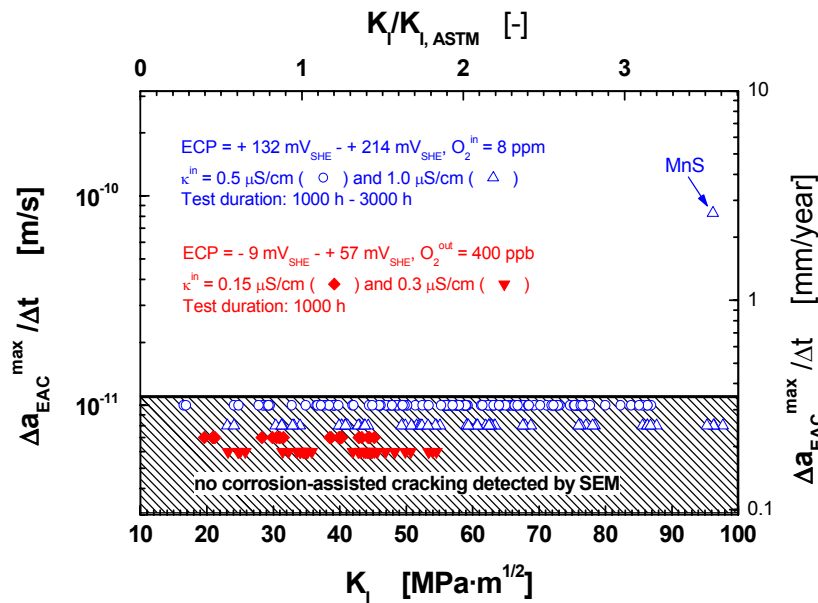


Figure 3: Summary of SCC CGRs from tests with WOL-DCB specimens in oxygenated HT water with different levels of sulphate [7].

Since the specimens were loaded outside the autoclave by insertion of a wedge, the very low susceptibility to SCC found in these constant-displacement testing under well-controlled conditions is most likely due to the almost complete exhaustion of low-temperature creep relaxation (and therefore absence of any significant crack-tip strain rate) before exposure of the specimens to environmental conditions promoting SCC [7].

SCC in Tests with Controlled Active Load: For K_I values < 50 to $60 \text{ MPa}\cdot\text{m}^{1/2}$ all C & LAS revealed a very slow susceptibility to sustained SCC crack growth in BWR/NWC environment in the temperature range from 274 to $288 \text{ }^\circ\text{C}$ with SCC CGRs well below 0.6 mm/year (Figure 4a) as long as the Vickers hardness/steel sulphur content were limited to values $< 350 \text{ HV5}$ and $< 0.02 \text{ wt.}\%$ and the water chemistry was maintained within current BWR/NWC operational practice ($< \text{EPRI action level 1}$, see Table 3). In combined slow rising-constant load or low-frequency fatigue-constant load experiments in high-purity or even sulphate-containing oxygenated HT water, where the constant load phase started with an actively growing transgranular (TG) EAC crack ($3\cdot 10^{-10}$ to $3\cdot 10^{-7} \text{ m/s}$), the SCC CGR either slowed down to CGRs of less than 0.6 mm/year or arrested within a few hundred hours under constant load in case of K_I values below $60 \text{ MPa}\cdot\text{m}^{1/2}$. Above $60 \text{ MPa}\cdot\text{m}^{1/2}$ the SCC CGRs tended to increase with increasing K_I values, although in many cases they were still decaying with time following roughly a reciprocal time law. Under reducing PWR or BWR/HWC conditions no sustained SCC crack growth was observed up to very high K_I values close to $100 \text{ MPa}\cdot\text{m}^{1/2}$ (Figure 4b).

Fast SCC was only observed under some very specific conditions, which usually appear atypical for current BWR and PWR power operation practice or properly fabricated and heat-treated modern C & LAS components. Combinations of several of the following unfavourable factors can lead to sustained fast SCC:

- A high corrosion potential $\text{ECP} > +100 \text{ mV}_{\text{SHE}}$ /high DO ($\gg 200 \text{ ppb}$) and quasi-stagnant flow conditions.
- $\text{Cl}^- > \text{EPRI action level 1 limit}$, $\text{SO}_4^{2-} \gg \text{EPRI action level 3 limit}$.
- A high steel S-content ($> 0.020 \text{ wt.}\% \text{ S}$).
- A high susceptibility to dynamic strain ageing (DSA) in connection with temperatures between $180 - 270 \text{ }^\circ\text{C}$.
- A high hardness/yield stress level ($> 350 \text{ HV5}$, $R_p > 800 \text{ MPa}$).
- Ripple loading ($R \geq 0.95$) or relatively frequent periodical partial unloading (PPU).
- Loading close to K_{II} or severe violation of small-scale-yielding conditions.

Under these unfavourable conditions, SCC CGRs can achieve rather high values, even up to a few m/year . The high-sulphur SCC line of the GE model gives a good estimate of the upper bound SCC CGR under such parameter combinations.

The conservative character of the BWRVIP-60 SCC disposition line (DL) 1 for stationary, transient-free BWR power operation has been confirmed for 270 to $290 \text{ }^\circ\text{C}$ and RPV base ($\leq 0.02 \text{ wt.}\% \text{ S}$) and weld filler/HAZ materials (Vickers hardness $< 350 \text{ HV5}$) if the water chemistry is maintained within current BWR/NWC operational practice ($< \text{EPRI action level 1}$) and K_I value is below $60 \text{ MPa}\cdot\text{m}^{1/2}$ (Figure 4a). Even above $60 \text{ MPa}\cdot\text{m}^{1/2}$ most test results, in particular with low- and medium-sulphur RPV steels, were still below this curve. DL 1 may be slightly exceeded at intermediate temperatures ($180 - 270 \text{ }^\circ\text{C}$) in C & LAS which show a distinct susceptibility to DSA (Figure 5). Furthermore, sustained SCC with CGR significantly above DL 1 was observed at $288 \text{ }^\circ\text{C}$ when excessive hardness ($> 350 \text{ HV5}$) (e.g., in bad weld HAZs) was present in the steel, in particular in combination with a high steel sulphur content (Figure 5). Under reducing PWR or BWR/HWC (Figure 4b) conditions no or very slow SCC crack growth well below the BWRVIP-60 SCC DL 1 was observed up to very high K_I values close to $100 \text{ MPa}\cdot\text{m}^{1/2}$.

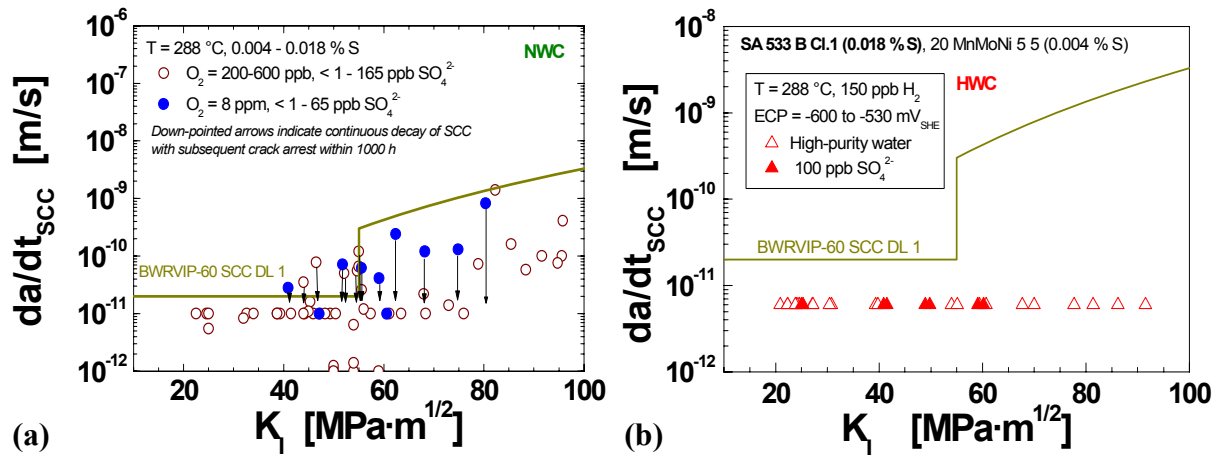


Figure 4: Confirmation of the conservative character of BWRVIP-60 SCC DL 1 for stationary, transient-free BWR/NWC (a) and HWC (b) power operation by combined slow rising load/low-frequency fatigue-constant load tests in chloride-free, oxygenated HT water at 274 to 288 °C [4, 9].

Control Parameter	Action Level 1	Action Level 2	Action Level 3
Conductivity [$\mu\text{S}/\text{cm}$]	> 0.3	> 1.0	> 5.0
Sulphate [ppb]	> 5	> 20	> 100
Chloride [ppb]	> 5	> 20	> 100

Table 3: Summary of action levels for reactor water during stationary BWR operation from EPRI BWR water chemistry guidelines [10, 11]. Apart from action level 2 for HWC, which is 50 ppb, the Swedish guidelines [12] are identical to those of EPRI.

The BWRVIP-60 SCC DL 2 for water chemistry or load transients conservatively covered the SCC crack growth during very severe sulphate transients relevantly above the EPRI action level 3 limit or under PPU conditions with constant load hold times > 5 to 20 h in both oxygenated (BWR/NWC) and hydrogenated HT water (BWR/HWC) [4, 9]. Under highly oxidizing BWR/NWC conditions ($\text{ECP} \geq +50 \text{ mV}_{\text{SHE}}$), DL 2 may be significantly exceeded during chloride transients > 5 to 10 ppb or in case of ripple loading ($R > 0.95$) in the frequency range from 10^{-3} to 0.1 Hz, even at fairly low stress intensity values around 20 to 30 $\text{MPa}\cdot\text{m}^{1/2}$ (Figure 5b). After severe (≥ 15 ppb) and prolonged (≥ 200 h) chloride transients, sustained SCC with a CGR above DL 2 was also observed in preliminary tests for a significantly longer time interval than the 100 h period specified in BWRVIP-60. Under reducing BWR/HWC conditions, on the other hand, the SCC CGRs during chloride transients of 100 ppb (= EPRI action level 3 limit) and under ripple loading were conservatively covered by DL 2.

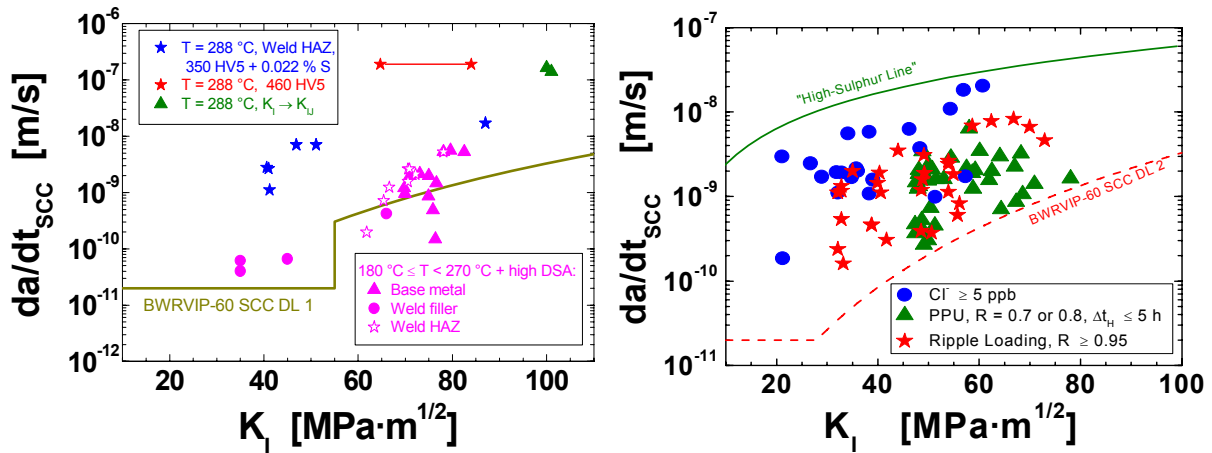


Figure 5: Test results with SCC CGRs above the BWRVIP-60 SCC DLs 1 and 2 [4, 9].

3.1.4 SCC Crack Growth During and After Chloride Excursions

BWRs are normally operated with neutral high-purity (< 1 ppb sulphate and chloride) water, but BWR operation also inevitably involves periodic short-term variations in water chemistry and ECP. Water chemistry and ECP transients occur during start-up/shut-down and occasionally during steady-state power operation (e.g., ion exchanger resin intrusions, condenser leakages, etc.). Therefore, the SCC crack growth behaviour of C & LAS during and after chloride or sulphate transients is of practical interest and relevance.

Even very high sulphate contents of up to 1400 ppb well above the EPRI action level limit 3 were not sufficient to induce accelerated SCC crack growth at K_I levels < 60 $\text{MPa}\cdot\text{m}^{1/2}$ under highly oxidizing BWR/NWC conditions and SCC rates were conservatively covered by the BWRVIP-60 SCC DL 2 [4, 9, 13]. On the other hand, recent PSI investigations clearly revealed that the addition of very small amounts of chloride as NaCl or HCl in the range of 5 to 15 ppb (slightly above the EPRI action level limit 1, see Table 3) were already sufficient to induce fast SCC crack growth in RPV steels well above the BWRVIP-60 SCC DL 2 under oxidizing BWR/NWC conditions ($\text{ECP} > 0 \text{ mV}_{\text{SHE}}$) down to very low stress intensity factors of 20 $\text{MPa}\cdot\text{m}^{1/2}$ (Figures 6 to 8) [4, 14 – 16].

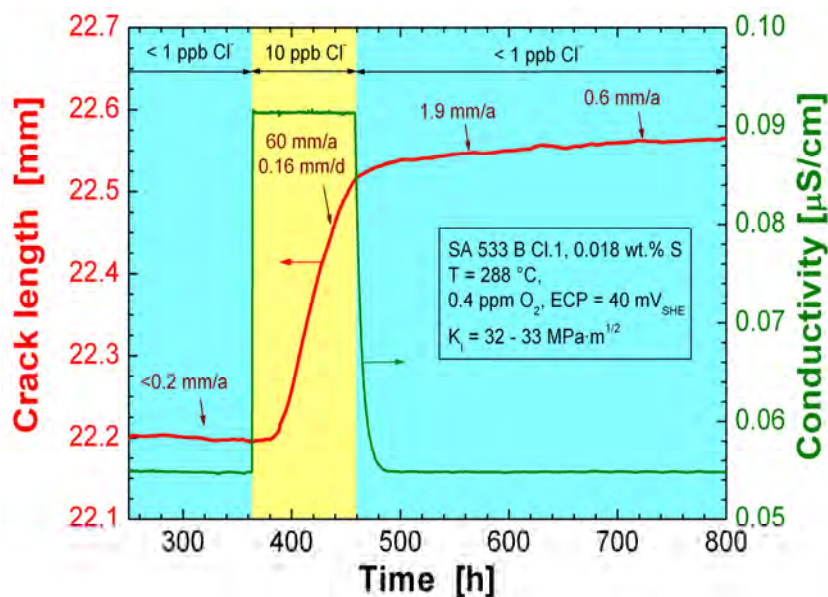


Figure 6: SCC crack growth before, during and after a 4 day chloride transient of 10 ppb (added as NaCl) in the reactor pressure vessel steel SA 533 B Cl.1 (0.018 wt.% S) under simulated BWR/NWC conditions.

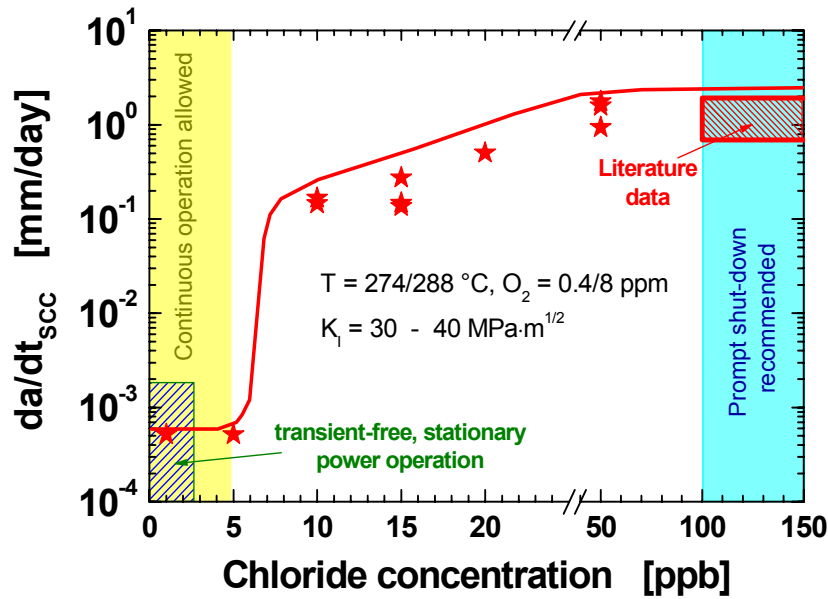


Figure 7: Effect of chloride concentration on SCC CGRs in high-sulphur reactor pressure vessel steels under highly oxidizing BWR/NWC conditions ($ECP = +50$ to $+150$ mV_{SHE}) and comparison with action level 1 and 3 range of the EPRI water chemistry guidelines. These investigations indicate a critical chloride concentration in the range of 5 to 10 ppb slightly above the action level limit 1 for the investigated reactor pressure vessel steels in the stress intensity factor range of 30 to 40 $MPa \cdot m^{1/2}$.

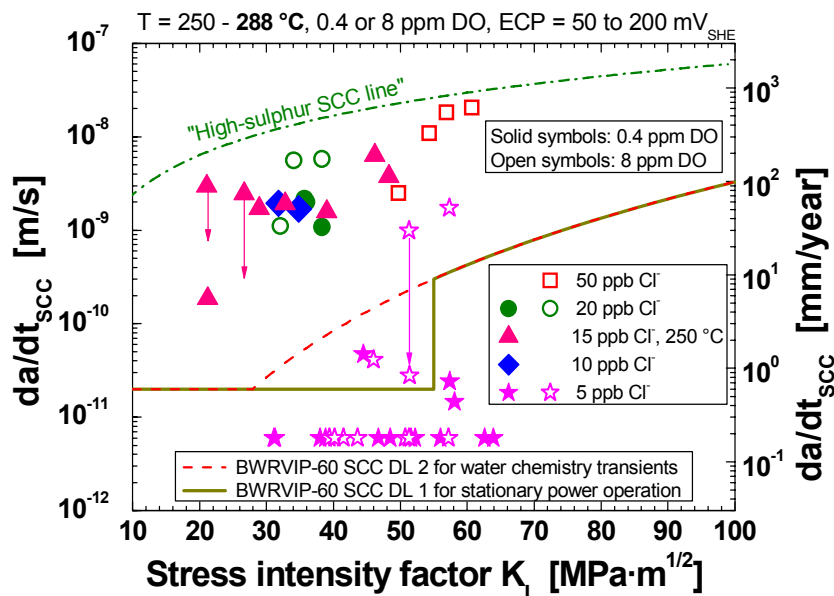


Figure 8: Comparison of SCC CGRs during chloride transients under BWR/NWC conditions with the corresponding BWRVIP-60 SCC DLs 2 and 1 for water chemistry transients and stationary power operation. Under highly oxidizing conditions the BWRVIP-60 SCC DL 2 is not conservative for chloride contents ≥ 5 ppb.

In constant load tests with PPU (to 80 % of maximum load every 12 h), acceleration of SCC crack growth was already observed a few hours after the addition of chloride in some cases. The stationary SCC CGRs during the chloride transients reached up to 1.5 mm/day at high chloride levels of 50 ppb and significantly exceeded the BWRVIP-60 SCC DL 2 for wa-

ter chemistry transients for chloride concentrations ≥ 5 ppb (Figure 8). In pure constant load tests with a non-growing “dormant” crack in high-purity water, a single partial unloading/reloading cycle was sufficient to induce fast SCC during the chloride transient.

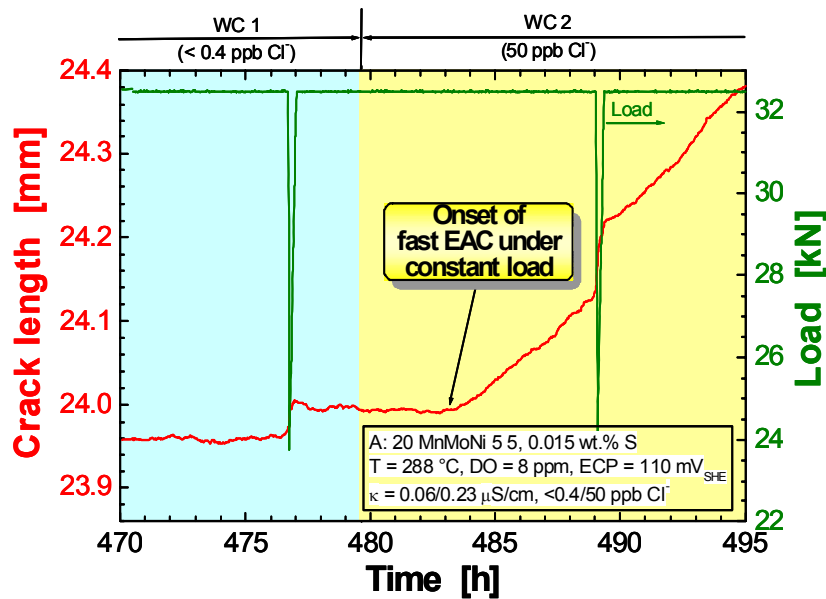


Figure 9: Onset of accelerated SCC during constant load phase three hours after the addition of 50 ppb of chloride to the oxygenated HT water in a test with PPU.

After returning to high-purity water, the cracks were still growing with the same high CGRs for some 10 to 50 h before a decay of the crack propagation rate was observed. In case of moderate chloride transients (≤ 10 ppb), the SCC CGRs then dropped again to the same low values as in high-purity water (< 0.6 mm/year) and below the BWRVIP-60 SCC DL 1 for transient-free, stationary power operation within some few further hundreds of hours. After severe (≥ 15 ppb) and prolonged (≥ 200 h) chloride transients sustained, fast SCC crack growth was observed for at least 1000 h (Figure 10).

The critical chloride concentration for the onset of accelerated SCC significantly increased with decreasing ECP. This result thus indicates a significantly higher impurity tolerance at lower ECPs (e.g., in the feedwater piping system) or under HWC conditions (Figure 11). The critical ECP for accelerated SCC, on the other hand, strongly increased with decreasing chloride concentration.

Although the observations are only valid for long pre-existing cracks, where enrichment of chloride in the crack-tip electrolyte by ion migration occurs [14 – 16] and may therefore not be directly transferred to defect-free component surfaces, they clearly show that much smaller chloride concentrations than believed so far can have a tremendous impact on SCC and that it is essential to maintain a low impurity level, in particular at high ECP under NWC conditions. The possibly short incubation period for acceleration of SCC in combination with the very high SCC CGRs under static loading conditions of up to 1.5 mm/day and possible long-term effects, at least after severe (≥ 15 ppb) and prolonged (> 200 h) chloride transients, arise some concern for severe chloride transients under BWR/NWC conditions. The frequency and extent of chloride transients above the EPRI action level limit 1 should therefore be reduced to the lowest possible level by adequate countermeasures and immediate actions.

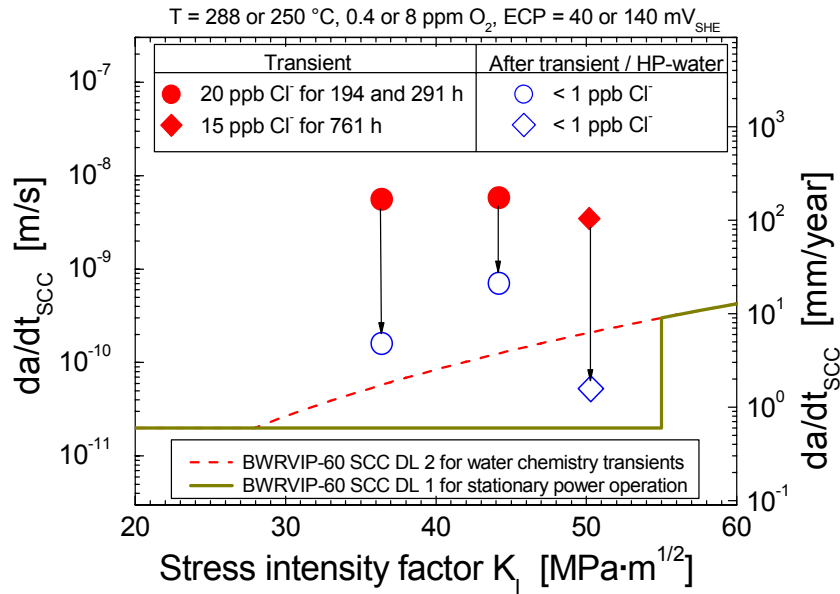


Figure 10: Test results with sustained stationary SCC in high-purity water during the whole remaining test period of up to 1200 h after severe (≥ 15 ppb) and prolonged chloride excursions (≥ 200 h).

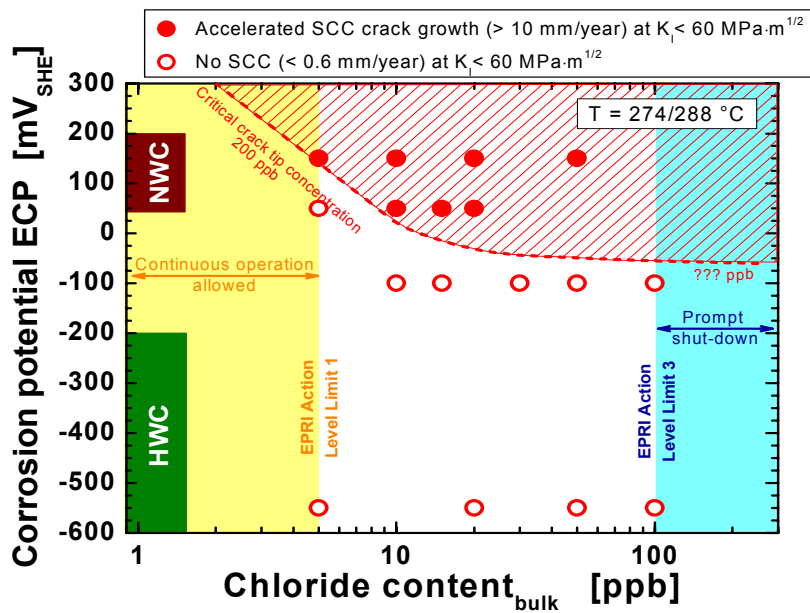


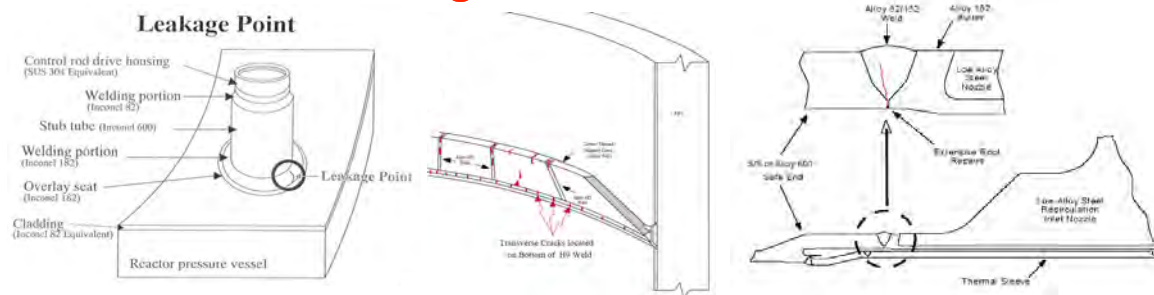
Figure 11: Synergistic effect of ECP and chloride content on the onset of fast SCC crack growth in reactor pressure vessel steels under BWR conditions and comparison with the typical conditions during stationary power operation (increasing chloride tolerance with decreasing ECP).

3.2 SCC in Dissimilar Weld Joints

3.2.1 Service Experience

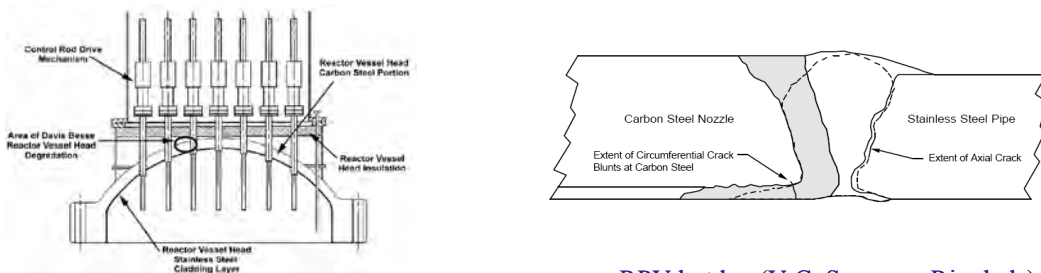
Inconel 182 has been widely used to join the LAS RPV and PV nozzles to both nickel-base wrought alloys (Alloy 600) and austenitic stainless steel (304L, 316L, 316NG) components in LWR by manual shielded metal arc welding (SMAW). In recent years, incidences of SCC in Inconel 182 in both BWR [17] and pressurized water reactors (PWR) [18] have been reported in some countries (Figure 12) and SCC susceptibility of uncreviced Inconel 182 weld material has been confirmed by laboratory investigations for both simulated BWR [19] and primary PWR coolant environment [20]. In the case of BWRs, components such as different nozzle safe ends [17], bottom head penetration housings [21] and core shroud support welds [22] have suffered from SCC. The BWR cracking was ID/intergranular (IG), often axial in nature and usually confined to the weld metal. None of the SCC cracks significantly penetrated the adjacent RPV base metal, which is consistent with the very high SCC resistance of LAS under BWR conditions [4]. Even after post-weld heat treatment (PWHT) relevant residual stress is observed in such weld joints and, in particular in the context of repair welding, it played a major role in many of these SCC incidents. The weld shrinkage strain/residual stress profile and the solidification structure (dendrite orientation) were important factors controlling the SCC crack path in weld joints. Cold-worked surface layers (e.g., from grinding) might further increase SCC susceptibility.

Boiling Water Reactors



Control rod drive housing (Hamaoka) Core shroud support structure (Tsuruga) Safe ends (Chinsan, ...)

Pressurized Water Reactors



Control rod drive housing (Davis Besse, Oconee, ...)

RPV hot leg (V.C. Summer, Ringhals)

Figure 12: Examples of SCC cracking incidents in dissimilar weld joints [17 – 22].

RPVs usually have a duplex (AISI 308L or 309L) or stabilized (X6 CrNiNb 18 10 \approx AISI 347) stainless weld overlay cladding. SCC in properly fabricated stainless steel weld overlay claddings has not been observed so far. Both stainless steel types usually show a high resistance against IGSCC. IGSCC has been observed in AISI 308/308L claddings (often in regions with manual or repair welding) in some few cases, which were clearly related to manufacturing and welding deficiencies (e.g., low delta ferrite content, extensive dilution and strong car-

bon pick-up resulting in sensitization or martensite formation and high hardness, high residual stress, extensive cold-work due to incorrect grinding) and other unusual circumstances [23 – 25]. None of these cracks [23 – 25] relevantly penetrated to the adjacent low-alloy RPV steels, and usually rather pitting- or crevice-like corrosion was observed at the stainless/LAS interface. Hot cracking in the stainless steel cladding and reheat or relaxation underclad cracks in the RPV steels were also observed in some cases. TG high-frequency thermal fatigue cracks have been observed in the feedwater nozzle corners of some GE BWRs because of a bad thermal sleeve design, which allowed a leakage flow of cold feedwater in the annulus between the nozzle and the sleeve. These cracks then further propagated to the RPV steel by SICC due to low frequency thermal and pressurization cycles associated with, e.g., start-up/shut-down and feedwater on-off cycles, scrams, or turbine rolls [26].

Because of the good service experience with stainless steel claddings and the results of the SCC tests in Oskarshamn 3, the SCC behaviour in Inconel 182 dissimilar weld joints and the cracking behaviour in the interface region between the Inconel 182 weld metal and low-alloy RPV base metal is further discussed in the next Section.

3.2.2 SCC in Inconel 182 Dissimilar Weld Metals

The extent and quality of the available SCC data in nickel-base weld metals of dissimilar weld joints are very limited, in spite of the practical importance of SCC of these weldments. Most investigated specimens were from simplified weld configurations or weld overlays, which might have a different microstructure. Most investigations were related to crack growth and bulk weld metal [19, 20, 27 – 43] and little attention has been paid to the interface region between Inconel 182 and LAS. The EAC susceptibility of dissimilar welds has been screened by slow strain rate tests with smooth tensile specimens [44 – 48]. It is not surprising that EAC was observed in all regions under adequate testing conditions: TG SICC, e.g., occurred in the LAS in oxygenated HT water and its severity was strongly dependent on the steel sulphur content. As expected, IG/ID SCC was observed in Inconel 182 weld metal in both BWR and PWR chemistries. In several cases interface cracking along the fusion line, often in conjunction with high hardness of the interface region, has been reported, thus indicating a distinct SCC susceptibility of this region.

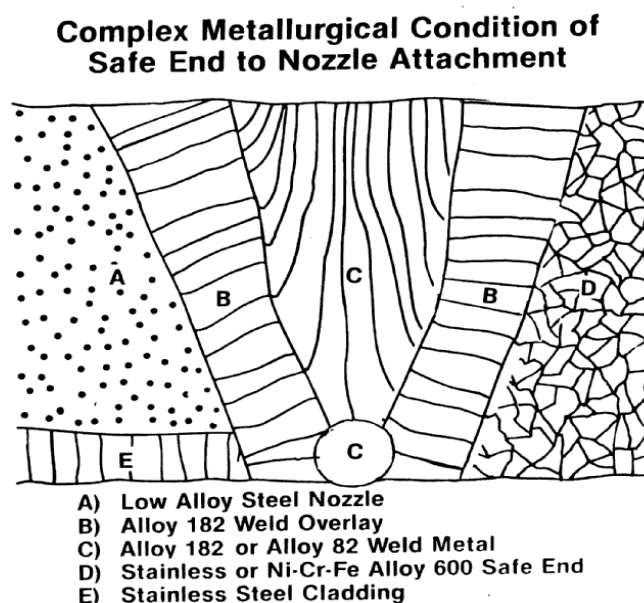


Figure 13: Example of complex weld configuration of a safe end to nozzle dissimilar weld.

Specific Metallurgical Features of Dissimilar Weld Joints and of the Inconel 182/LAS Interface with Respect to EAC: Multipass dissimilar weld joints usually have a complex welding configuration (Figure 13) and microstructure. The general structure of an individual weld pass consists of elongated dendrites at the edge of the melt pool, where heat transfer is highly directional, and equiaxed dendrites in the middle with slower cooling (Figure 14). During solidification, the dendrite arms grow towards each other and trap “enriched liquid” (e.g., by low melting compounds, Mn, Nb, S, P, Si) in the interstices along with melt oxides. Therefore, the dendrite boundaries are often decorated with precipitates and enriched with sulphur/phosphorous. Each weld pass heats up the layers below and can cause recrystallization, segregation (S, Mn, Si), precipitation (e.g., carbides) or hot cracking and produce a wide range of microstructures potentially susceptible to EAC. PWHT or in-service ageing can further exacerbate EAC susceptibility.

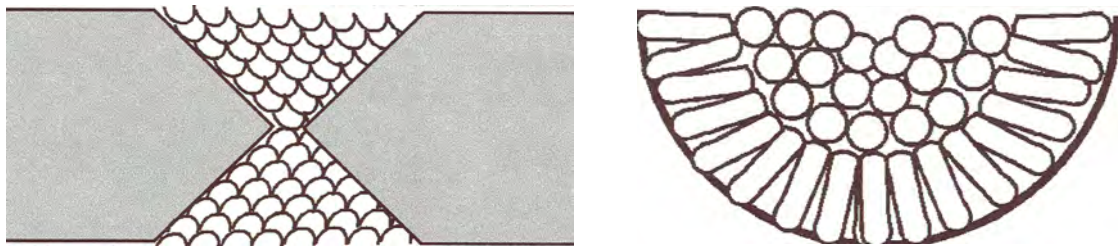


Figure 14: Schematic of solidification structure in individual weld pass.

The situation is even more complex close to the LAS interface, where the dilution of alloying elements between Inconel 182 weld filler and LAS base metal during welding or the migration of carbon from the LAS to the weld metal during PWHT may produce even more complex microstructures. Usually, in the weld metal close to the fusion line, a few mm thick zone with different chemical composition from the mixing of the weld filler material with the molten LAS is observed (Figure 16). The reduced chromium (and nickel) content in this dilution zone close to the LAS tends to increase its corrosion and SCC susceptibility (e.g., by the effect of chromium on the repassivation behaviour) with respect to the bulk weld metal. In case of very high dilution between the Inconel 182 weld metal and the LAS, e.g., the local formation of a very narrow and hard layer of martensite on cooling in the weld metal adjacent to the fusion boundary is possible, but this can be tempered by the PWHT and by the adjacent weld runs (this aspect is more characteristic for stainless steel weld metals, where significantly less dilution is required to form martensite). Sulphur and phosphorous segregation to intercolumnar/ID boundaries may occur during solidification and PWHT, in particular in case of welding consumables, which have a high sulphur and phosphorous content, and thus result in an increased SCC susceptibility [31 – 33]. Carbon migration from the LAS to the weld metal, in particular during PWHT, can result in the precipitation of chromium-rich carbides resulting in an increase in hardness/yield stress and chromium-depleted grain boundaries/sensitized microstructure and therefore in an increased SCC susceptibility. A further consequence of carbon diffusion is that the LAS may become decarburized in a zone adjacent to the fusion boundary in severe cases. This decarburized zone may be softer and may have a lower yield stress than the parent LAS, and therefore a potentially higher susceptibility to SICC during plant transients. The LAS weld HAZ of dissimilar weld joints usually has a lower peak hardness (≤ 300 HV5) than in welds between LAS components (≤ 350 HV5) (Figure 17). Furthermore, the different thermal expansion coefficient of Inconel 182 and LAS may produce relevant thermal stress at the interface during start-up/shut-down and also at operating temperature and thus result in a change of the acting stress intensity factor. Significant galvanic effects are not expected, since the ECP of the LAS in BWR/NWC environment is only slightly smaller (50 to 100 mV) than that of Inconel 182 and since the throwing power is very limited in high-purity (very low conductivity) water.

SCC Behaviour of Bulk Inconel 182 Weld Metal: The possibility of SCC crack growth in uncreviced bulk Inconel 182 weld metals in high-purity BWR and PWR environment has been demonstrated both by laboratory investigations [19, 20, 27 – 43] and service experience [17, 18]. The extent and quality of the available SCC data in Inconel 182 weld metals are relatively limited and subjected to tremendous scatter. This scatter in the data is substantially the result of data quality issues, such as specimen machining, fatigue pre-cracking, transitioning from the TG pre-crack to an IG/ID SCC crack, crack measuring anomalies associated with highly uneven crack fronts, inaccurate control and measurement of corrosion potential and water purity, etc.

The SCC behaviour of Inconel 182 weld material and data trends are quite similar to those observed in Alloy 600 or stainless steels, although the higher HT yield stress of Inconel 182 may make it more susceptible to SCC (steeper strain gradient and higher crack-tip strain rate) and low-temperature rapid crack propagation, and produce high weld residual stresses and stress intensity factors [19]. Because of the good creep/relaxation resistance of Inconel 182, PWHT does not completely eliminate weld residual stress and even in the adjacent RPV steel relevant residual stress can prevail after PWHT. PWHT can produce some elevation in yield strength and potentially exacerbate Cr depletion (both by carbide precipitations), while reducing some of peaks in residual stress [19]. As-welded structures can be regarded as solution-annealed and weld joints with PWHT as sensitized. ID (sulphur/phosphorous segregation) and grain boundary chemistry of weld metals may be markedly different than wrought materials and contribute to SCC [19, 46, 49]. Maximum susceptibility/SCC growth rates are usually observed, if maximum stress/crack growth direction is perpendicular/parallel to main dendrite axis [19]. Hot cracking (or grain boundary weakening) occurs in some heats and welds of Inconel 182 weld metal (in particular with high Si content). While it contributes to the loss of integrity, it must also be carefully isolated from SCC. For certain combinations of temperature and H₂ content (PWR) the Inconel 182 weld metal may be shifted to the thermodynamic Ni⁰-stability region in the potential/pH-Pourbaix diagram, which reduces the SCC CGRs [19].

Recent investigations under well controlled conditions [19, 32] revealed less scatter and a more reproducible behaviour (Figure 15). The experiments in [19] showed very similar parameter trends (for the effect of ECP, sulphate/chloride, cold work, sensitization, stress intensity factor, etc.) as in stainless steels. SCC rates in Inconel 182 under HWC conditions were usually significantly lower (typically by a factor of 5 to 10) than under NWC conditions. Unlike sensitization, which elevated SCC growth rates only at a high ECP, cold work elevated the CGRs at both high and low corrosion potentials. Investigations with different heats representing good quality welds revealed no significant heat to heat variation or differences in SCC growth rates between the as-welded or PWHT conditions. In another investigation [32, 33], on the other hand, SCC rates were enhanced by high concentrations of phosphorous and sulphur in clean (sulphate-free) BWR/NWC environment, but not in environments with sulphate additions. A low concentration ratio of stabilization elements like Nb and Ti to C (stabilization ratio) slightly enhanced SCC CGRs [32, 33]. The beneficial effect of HWC was larger in materials with low phosphorous and sulphur content than in welds that had a high content of these elements [32, 33].

SCC initiation in Inconel 182 weld and Alloy 600 wrought material was studied by bolt-loaded modified C(T) specimens with an U-notch and different notch-radii, which were exposed to BWR/NWC and HWC in Oskarshamn 3 and 2 over a period of 5 and 3 years, respectively [31, 34]. SCC initiated in a relevant fraction of the Inconel 182 specimens tested in NWC environment already during the first year of exposure, while the frequency of crack initiation was somewhat less in HWC environment. In Alloy 600 very little crack initiation occurred in NWC, and none was detected in HWC. The results of this study indicated that the

local chemical attack on grain or ID boundaries may act as initiation sites for SCC and SCC cracks were more prone to initiate under triaxial strain than under plane strain conditions, under similar principal stresses. Materials with high SCC CGRs also revealed the highest SCC initiation susceptibilities. Materials with a low stabilization ratio and high phosphorous or sulphur content revealed the highest SCC initiation and growth susceptibilities. SCC initiation susceptibility was highest in the as-welded conditions with respect to PWHT or thermally-aged conditions in this study.

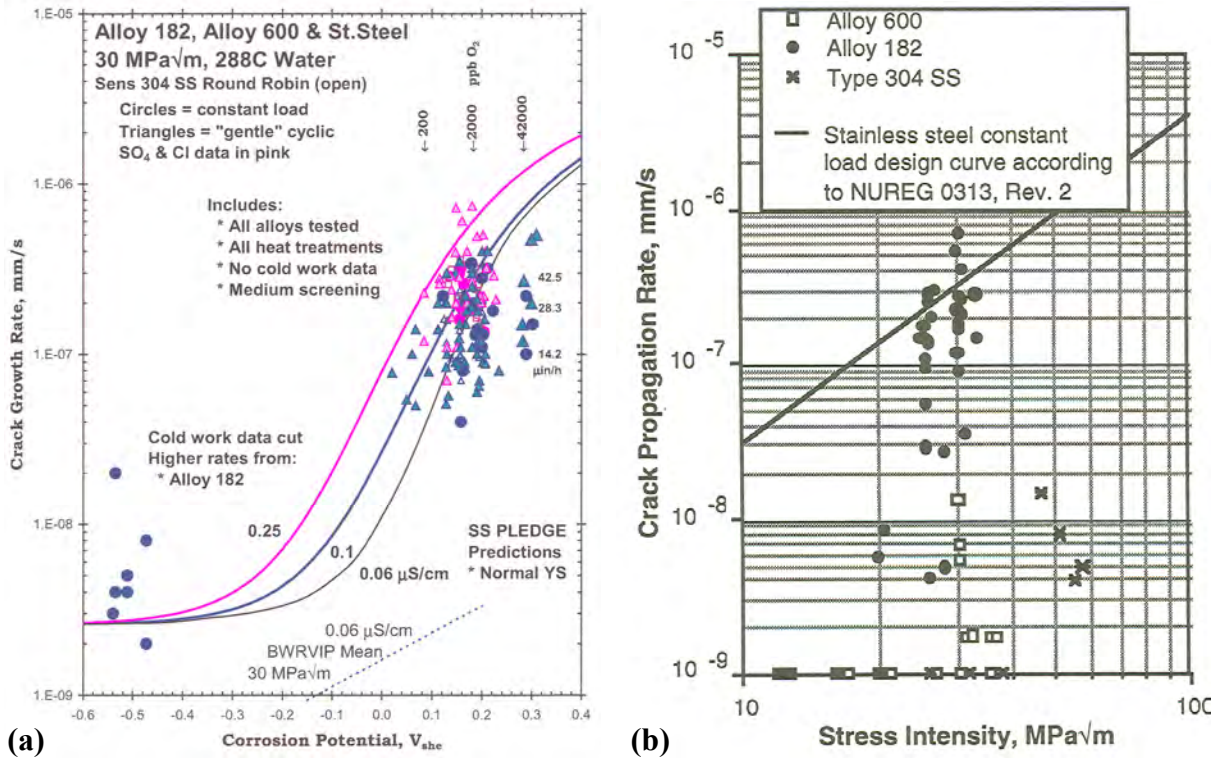


Figure 15: Effect of ECP on SCC CGRs in Inconel 182 weld metals (a) [19] and range of SCC CGRs of different Inconel 182 weld metals (b), which were subjected to BWR/NWC environment in Oskarshamn 3 [32, 33].

SCC Crack Growth Behaviour in the Dilution Zone and at the Inconel 182/LAS Interface:
 So far, a small ongoing collaboration between the Fracture Research Institute (FRI) of the Tohoku University and PSI has been the sole attempt to carefully study the SCC crack growth behaviour in the dilution zone and interface region of a simulated Inconel 182/SA 508 Cl. 2 weld joint under simulated BWR/NWC conditions in autoclave tests [50]. For this reason a weld joint of Inconel 182-SA 508 Cl.2 was manufactured by filling a rectangular groove in a forged RPV steel plate by manual multipass SMAW, which then was PWHT at 620 °C for 24.5 h. Chemical composition and microhardness profiles across the fusion line are shown in Figures 16 and 17. 25 or 12.5 mm thick compact tension C(T) specimens were cut in such a way, that the fusion line was lying in the remaining specimen ligament and perpendicular to the crack plane. The crack plane of the specimens was parallel to the main dendrite growth direction in the Inconel 182 weld material and perpendicular to the fusion line. The MnS-inclusions of the RPV steel were parallel to the pre-crack front and fusion line. The specimens were then fatigue pre-cracked in air at room temperature and the tip of the fatigue pre-crack was located either in the bulk Inconel 182 weld metal or in the dilution zone. After fatigue pre-cracking, some specimens were 5 % side-grooved with a circular notch.

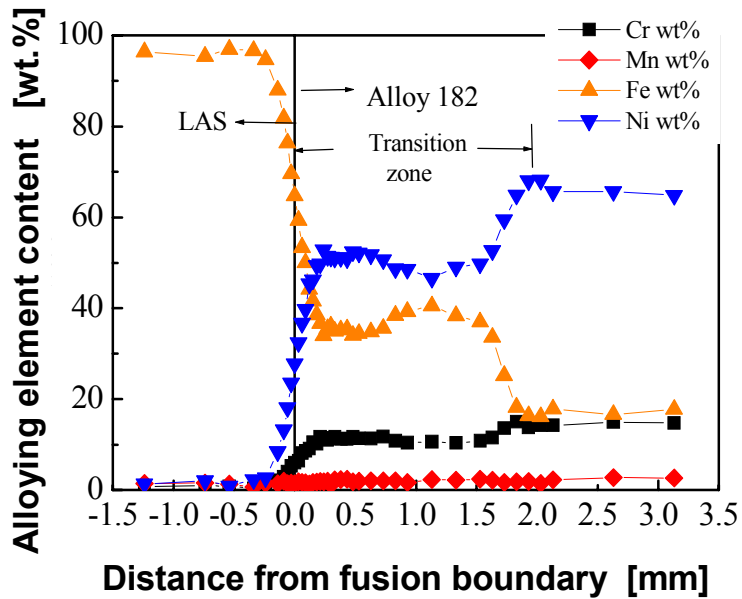


Figure 16: Chemical composition profile of selected alloying elements across the fusion line. The dilution zone in the weld metal adjacent to the fusion line with a different chemical composition than the bulk weld metal is formed by the mixing of the molten weld filler and RPV steel and had an extension of 1.5 to 2.5 mm.

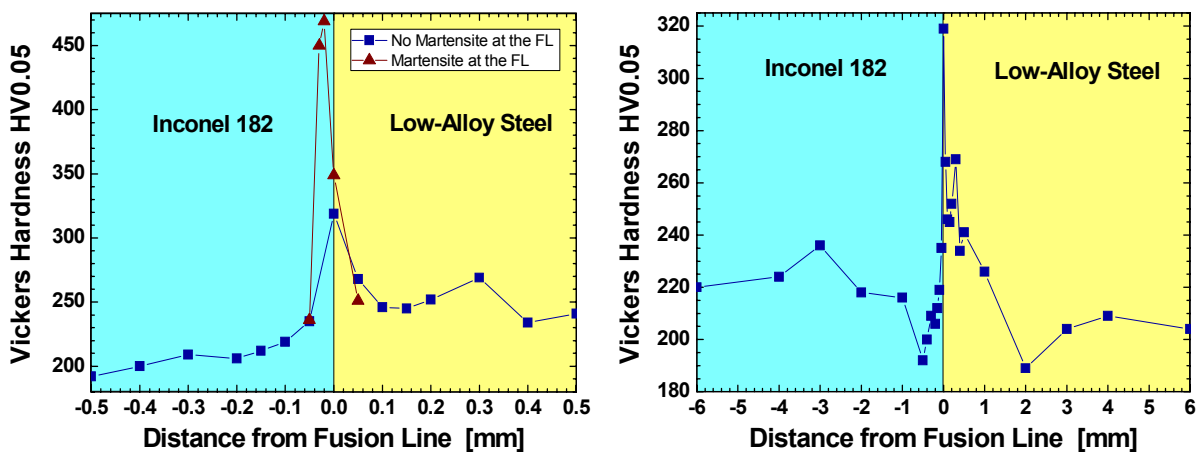


Figure 17: Typical microhardness profiles across the fusion line. The thickness of weld HAZ in the RPV steel had an extension of 2 to 4 mm and peak Vickers hardness was usually below 300 HV5. At some locations of the fusion line, a martensite-like or carbide-rich region with very high microhardness of up to 480 HV0.05 was observed.

The SCC behaviour was investigated under simulated BWR/NWC conditions in tests with PPU and static loading. The experiments were performed in stainless steel autoclaves with integrated tensile loading machines, which were attached to refreshing HT water loops. The crack growth was on-line monitored by the DCPD or ACPD method and verified by post-test fractography in the SEM. The tests were performed in oxygenated (0.2, 0.4, 2 or 8 ppm DO content), high-purity or 30 ppb sulphate-containing HT water at 288 °C.

After pre-oxidizing the specimens during 200 h at a small pre-load, an actively growing ID EAC crack was then generated by applying a triangular waveform loading with a load ratio R of 0.7, whereas the loading frequency was decreased in one step from 0.01 to 0.001 Hz. Then a trapezoidal waveform loading at R = 0.7 with a hold time of 9000 s was additionally

introduced. After this initial loading procedure, the loading mode was changed to PPU or near constant load (PPU with a holding time of 24 h). In some other tests loading consisted of several sequences of cyclic, PPU and static loading to study the crack growth behaviour in different microstructure regions of the weld joint. In order to reduce the total testing time, the applied stress intensity factor was stepwise increased in conjunction with SO_4^{2-} -addition and an increase of DO from 0.4 to 8 ppm.

These investigations revealed the following important results: As expected, fast ID SCC was observed in the Inconel 182 bulk weld metal in oxygenated, high-purity HT water in the typical range of other investigations (Figure 18). The subsequent SCC CGRs in the Inconel 182 dilution zone were similar to those of the bulk weld metal and tended to slightly decrease with decreasing distance to the fusion line (Figure 18).

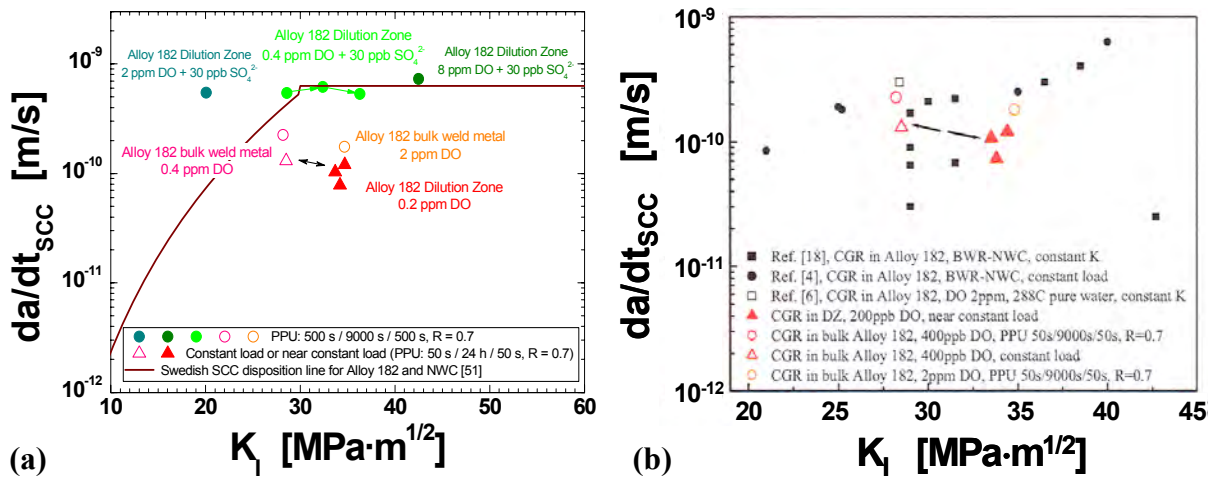


Figure 18: Similar SCC CGRs in the dilution zone and bulk weld metal of the weld joint [50] (a). The SCC CGRs are in the same range as in other comparable investigations under BWR/NWC conditions [19, 30, 36] (b).

Cessation of SCC was observed under PPU conditions for those parts of the crack front, which reached the fusion line. As soon as the overwhelming part of the crack front has reached the crack front, a drastic drop of ID SCC CGRs (Figures 19 and 20) was observed even under aggressive environmental conditions (8 ppm DO and 30 ppb SO₄²⁻) and crack arrest occurred at or close to fusion line under PPU/constant load (Figures 19 and 21).

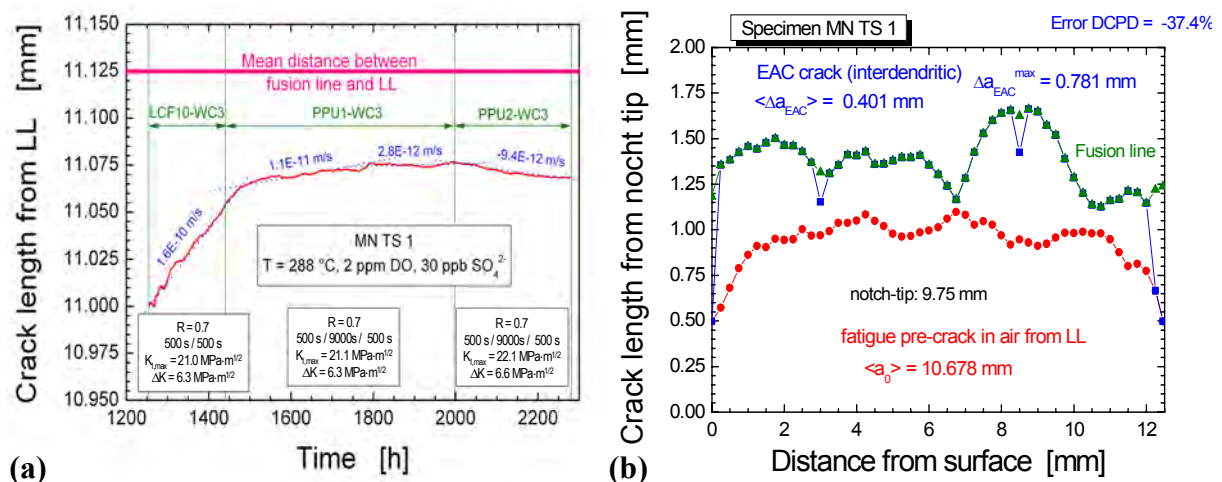


Figure 19: Cessation of SCC crack growth at the fusion boundary indicated by DCPD (a) and confirmed by post-test fractography (b).

Even in case of severe cyclic loading and aggressive water chemistry conditions, the cracks had problems to cross the fusion line and rather tended to grow in the Inconel 182 dilution zone along the fusion line before they finally entered into the RPV steel. This indicates an increased EAC susceptibility of the interface region parallel and close to the fusion line in the dilution zone of the weld metal. After crossing of the fusion line under severe cyclic loading conditions, the SCC CGRs under PPU in the LAS HAZ were more than one order of magnitude lower than in the Inconel 182 bulk weld material. Suddenly after switching from PPU to constant load, cessation of SCC and crack arrest occurred in both the LAS HAZ and bulk LAS in spite of the high applied stress intensity factors and aggressive environmental conditions. The Inconel 182 bulk weld material and the bulk LAS of the bimetallic weld joint specimen therefore behaved exactly in the same manner as corresponding materials in homogeneous specimens.

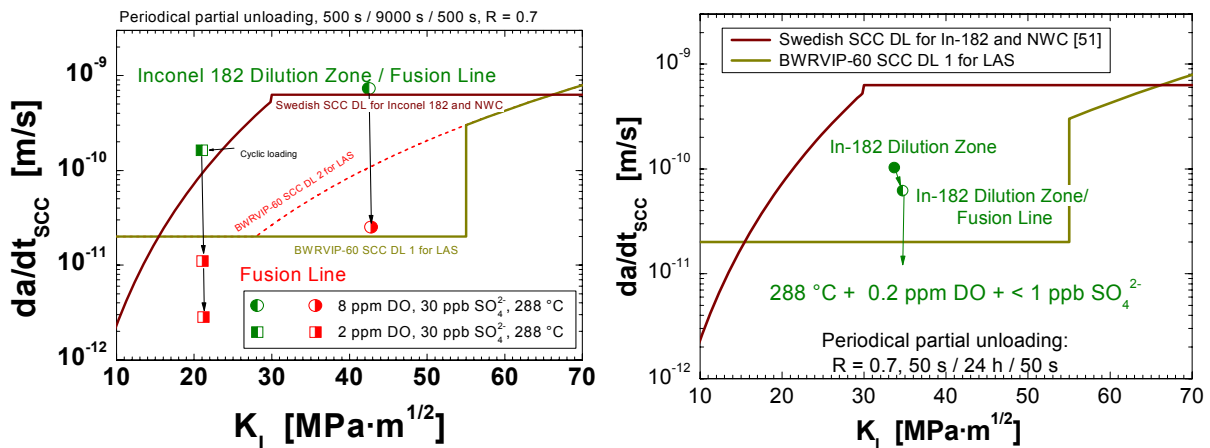


Figure 20: Comparison of SCC CGRs at the interface region with a Swedish DL for Inconel 182 weld metals (implemented by the Swedish utilities, [51]) and BWRVIP-60 SCC DLs for LAS [4].

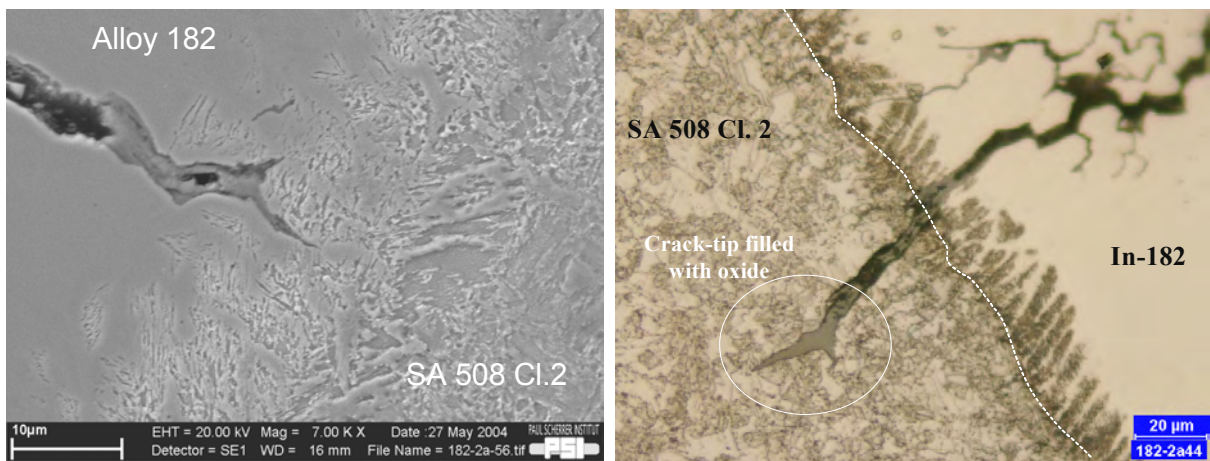


Figure 21: Confirmation of cessation of SCC at or close to the fusion boundary by etched cross sections. The Nital etching only attacks the LAS, but not the Ni-base weld metal.

These preliminary results correlate excellently with field experience, where SCC cracking was usually confined to the Inconel 182 weld metal [17, 18] and no cases of SCC were observed in C & LAS primary pressure boundary components [4]. The fusion boundary seems to represent a relevant barrier for SCC crack growth, but minor crack growth into the adjacent RPV steel is not impossible (as shown in Figures 21 and 27). Under static loading conditions

in chloride-free HT water, there seems to be little risk, that a fast growing ID SCC crack may cross the fusion line and relevantly propagate to the adjacent low-alloy RPV steel. Even if a crack would cross the fusion line under static load, it is anticipated that cessation of SCC occurs in the LAS HAZ or at latest in the unaffected LAS base material. Major EAC crack propagation to the RPV material is therefore not expected as long as the number of plant transients is limited and severe and prolonged chloride excursions are avoided (i.e., if water chemistry is kept below the EPRI action level 1 limit).

4 Evaluation and Assessment of the SCC Data from Oskarshamn 2/3

4.1 Relevance of Test Materials, Procedures and Conditions

4.1.1 Materials

The Swedish RPVs except Oskarshamn 1, Oskarshamn 3 and Forsmark 3 have been manufactured from ASTM A 533 B Cl.1 steel. In the two latest plants Oskarshamn 3 and Forsmark 3, forged rings of the material ASTM A 508 Cl.3 were used for the cylindrical shell. Inconel 182 was used as cladding material in Oskarshamn 2, Barsebäck 1 and 2 and Forsmark 1 and 2 for the bottom RPV region. In all other vessels, Type 308/309 stainless steels have been used.

The investigated RPV materials may be regarded as representative for modern Western RPVs of LWR and should conservatively bound the Swedish RPV steels, which usually have a lower steel sulphur content and a rather favourable morphology of MnS-inclusions [3, 52].

4.1.2 Applied Test Procedure

A slow positive (crack-tip) strain rate and sufficiently high tensile strain are essential for EAC initiation and subsequent growth in C & LAS in HT water [4]. Distinct positive/negative feedback and hysteresis effects on SCC crack growth can be observed in C & LAS, since a) the crack-tip strain rate is usually increasing with increasing K_I , dK_I/dt , dK_I/da , and CGR [53] and b) since crack-tip strain rate and environment are both dependent on CGR and vice versa [4, 54, 55]. Depending on loading mode (constant load vs. constant displacement) and K_I vs. a relationship for the used specimen or cracked component negative or positive feedback effects on SCC crack growth may be observed. During stationary power operation static loading of the RPV prevails and stress intensity factors increase with increasing crack length ($dK_I/da > 0$). During operational transients (start-up, etc.) with pressurization and thermal cycles, loading includes phases with slowly increasing stress intensity factors ($dK_I/dt > 0$). In passively bolt- or wedge-loaded specimens (constant COD tests), on the other hand, the stress intensity factor decreases with increasing crack extension ($dK_I/da < 0$). Since such specimens are loaded prior to exposure to the BWR environment, the crack-tip strain rate is virtually zero before crack initiation due to the almost complete exhaustion of low-temperature creep relaxation. Subsequent to heating-up, where some additional relaxation happens, no further dynamic crack-tip straining usually occurs. In this kind of specimen, it is rather difficult to initiate SCC, in particular under moderate environmental and loading conditions, and the probability for local crack pinning/cessation phenomena is higher than in actively loaded specimens. Passively loaded specimens might therefore feign a high resistance against SCC under certain conditions, where tests with active loading might reveal SCC. It is therefore essential, that a sufficient amount of specimens is tested over very prolonged exposure periods (which both were the case for the tests in Oskarshamn 2 and 3). A low SCC crack growth susceptibility should always be verified by some verification tests with controlled active load and triggering of EAC (e.g., by PPU or combined slow rising-/cyclic-constant load tests).

4.1.3 Test Conditions

The environmental test conditions over the exposure period of five (NWC) and four (HWC) years may be regarded as characteristic and representative for current BWR/NWC and HWC nuclear power operation. During the third year of testing under NWC conditions, there was a significant chloride excursion of 5 to 30 ppb during a period of three weeks because of a condenser leakage briefly after an outage. As discussed in Sections 4.2 and 4.3, this might have affected the cracking behaviour.

With respect to a postulated semi-elliptical surface crack, which penetrates the Inconel 182 or stainless steel 308/309 cladding and reaches to the RPV steel, the ECPs on the low-alloy RPV steel specimens in the test loops are expected to be 50 to 100 V lower under NWC conditions. Therefore, testing conditions are slightly less aggressive than within the reactor. This is due to the fact that LAS have an ECP which is usually 50 mV lower than that of stainless steels or Ni-base alloys and due to the presence within the RPV of other oxidizing species than O_2 , particularly H_2O_2 , which might result in an additional slight shift in ECP at comparable total oxidant ($O_2 + \frac{1}{2} H_2O_2$) concentrations in the range of 200 to 600 ppb DO content. Because of the heterogeneous (at component surfaces) and homogeneous decomposition of hydrogen peroxide to oxygen and water, the highest concentration of H_2O_2 is postulated to exist in the coolant within the reactor core zone. A decrease in concentration proportional to the distance travelled by the coolant after exiting the reactor core is expected for the remaining water containing regions within the RPV. Therefore, significantly lower H_2O_2 concentrations might prevail in the test loops. The slightly smaller potential gradient in the crack mouth region might be partially compensated by the higher turbulent flow rate within the RPV.

4.2 Evaluation and Assessment of the Test Results

No major deficiencies in test procedures/test conditions nor indications for testing artefacts (e.g., overloading of specimens) or fabrications deficiencies/defects of specimens (e.g., excessive hardness of weld HAZ or atypical microstructure of RPV steel) could be found based on the available test documentation provided by SKI/ABB [2] and the metallurgical evaluations performed by VTT [3]. The test results may therefore be regarded as valid. Weld residual stress, which has not been measured, but which is partially eliminated by PWHT and specimen cutting, is just regarded as a minor factor, which can slightly change the K_I , but has not relevantly affected the test results [3].

The apparent very poor correlation between post-test fractography and DCPD measurements was most probably related either to the fact that in most cases the real crack advance and DCPD indications were below or in the range of the DCPD accuracy of 0.3 to 0.5 mm in RPV steels or to crack bridging phenomena. Therefore, no reliable information on the course of crack growth during the exposure period was available. In those few cases with relevant crack advance, DCPD usually also indicated a relevant crack advance. In case of non- or slowly-growing cracks or crack arrest during the test period, relevant parts of the crack crevice can become filled with a magnetite oxide film (with good electronic conductivity), which is formed in the oxygen-depleted crack crevice. The oxide film, the precipitation of sulphides and other corrosion products during shut-down or Ni-precipitates in specimens with Inconel 182 cladding (if crack-tip pH, ECP and temperature are in the thermodynamic Ni-stability region) may act as conducting bridges between the crack flanks, which results in an apparent shortening of the crack in DCPD measurements, in particular in bolt-loaded specimens with low K_I values and small crack openings.

The investigations in Oskarshamn 3/2 generally revealed a low SCC crack growth susceptibility of RPV steels in realistic BWR environments. The apparent average SCC CGRs and crack advances in the RPV steels under NWC and HWC conditions are summarized in Figures 22 to 24. All non-cladded specimens and specimens with AISI 308L stainless steel cladding revealed no or only minor crack growth (< 0.24 mm) under both BWR/NWC and HWC conditions, which usually appeared as a ditch. Often 4 to 6 striation-like markings were seen in this zone sometimes in conjunction with some TG or IG features at the crack-tip, indicating that they may be connected to the annual interruptions of the test and some intermittent crack growth (e.g., during start-up) followed by general corrosion. The fracture surface was too corroded and the crack extension too small to enable reliable determination of cracking

mode. However, the specimens with Inconel 182 cladding and fatigue pre-crack in the weld metal revealed clear, but minor SCC crack growth into the HAZ of the RPV steel under BWR/NWC conditions. Marked SCC crack growth of 2.43 mm in the RPV steel was only observed in one of the Inconel 182 cladded specimens tested under BWR/NWC conditions with a high K_I value of $48.8 \text{ MPa}\cdot\text{m}^{1/2}$, where the fatigue pre-crack tip was located in the RPV steel base metal far beyond its HAZ. Detailed post-test fracto- and metallography confirmed that cracking in this specimen was due to SCC and it could be neither related to any mistreatment of specimen, welding defects, testing artefacts nor to any microstructural anomalies.

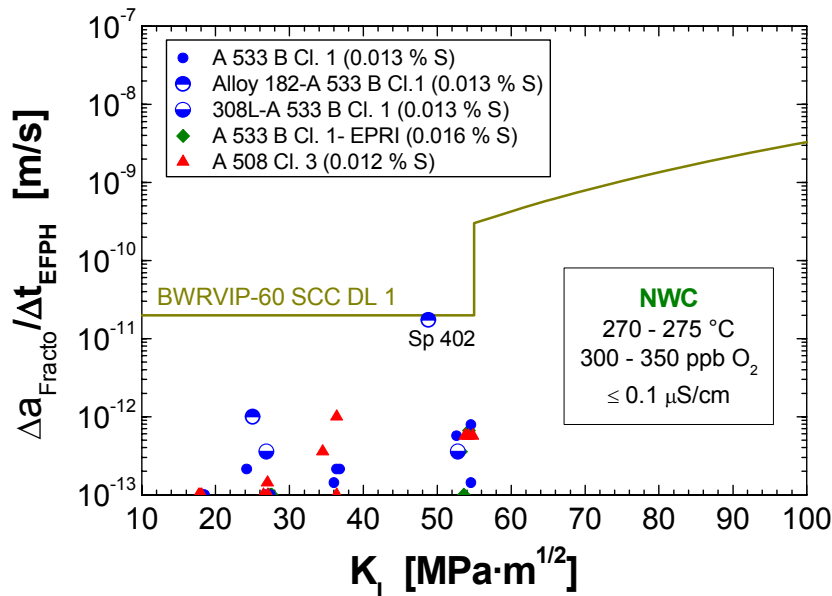


Figure 22: Comparison of average SCC CGRs in RPV steels under BWR/NWC conditions with BWRVIP-60 SCC DL 1.

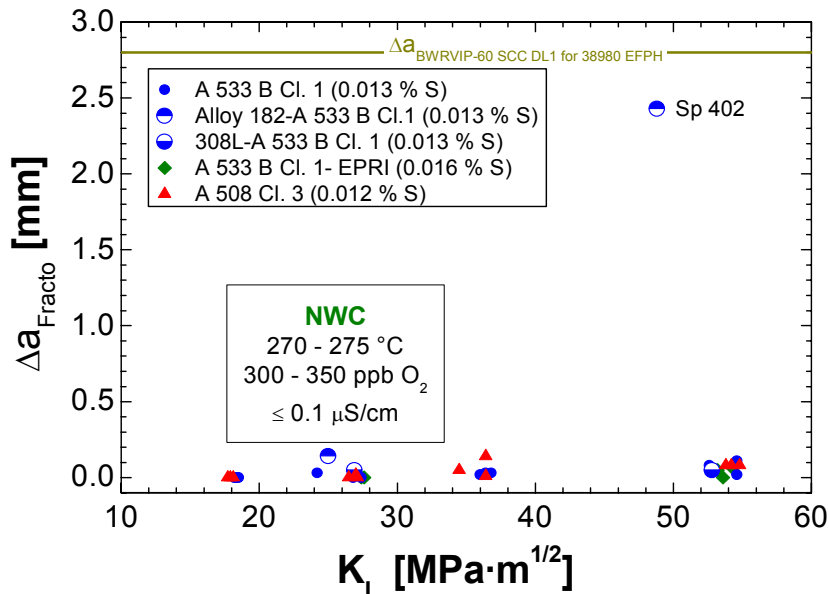


Figure 23: Crack advance in RPV steel during the five year exposure under NWC conditions in Oskarshamn 3. Apart from specimen 402, the crack advance were below or in the range of the accuracy of DCPD and smaller than 10 times the mean grain size.

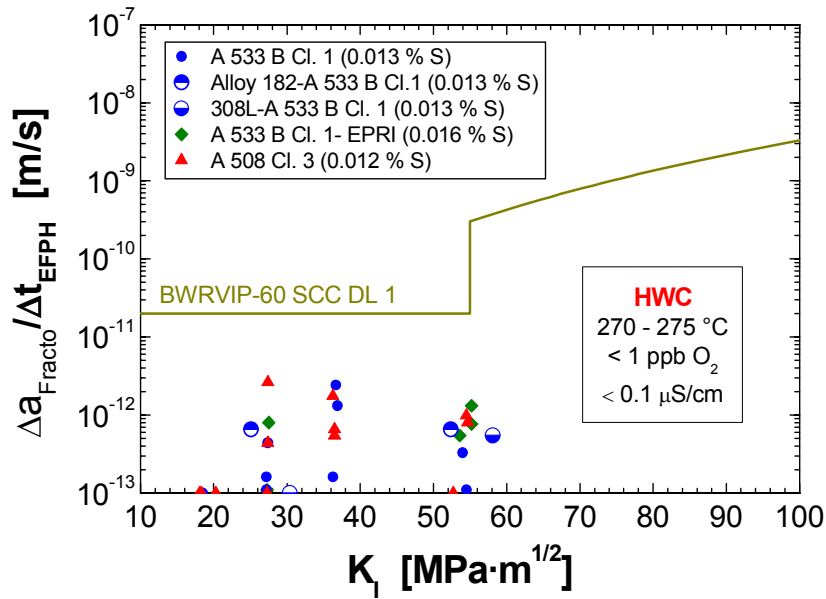


Figure 24: Comparison of average SCC CGRs in RPV steels under BWR/HWC conditions with BWRVIP-60 SCC DL 1.

As expected, ID SCC was observed in the Inconel 182 weld metal under BWR/NWC and HWC conditions, but with significantly slower CGRs under HWC conditions (Figure 25). Based on Ref. [31, 34], it can be assumed that the cracks probably initiated at an early stage of the exposure period. The apparent average SCC CGRs were within the lower range of typical SCC CGRs in Inconel 182 weld metals even if crack growth in LAS according to BWRVIP-60 SCC DL 1 was taken into account (Figure 25) or if it is assumed that the overwhelming part of SCC might have occurred during the first exposure year as indicated by DCPD for the higher loaded specimen 302. The lower bound SCC CGRs under NWC conditions might eventually be related to a good quality weld with a lower SCC crack growth susceptibility. An alternate explanation is that the growing crack already reached the fusion line at an early stage of the exposure period and then arrested in the weld HAZ of the RPV steel.

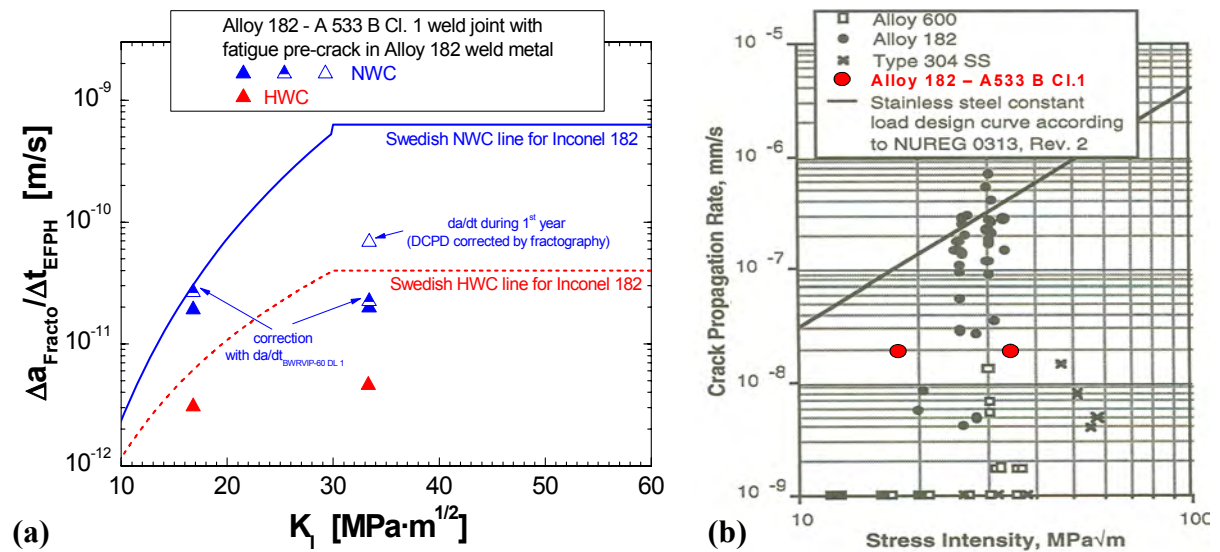


Figure 25: Comparison of average SCC CGRs in Inconel 182 weld metal with corresponding Swedish DLs for NWC and HWC conditions (implemented by the Swedish utilities, [51]) (a) and with SCC CGRs from bolt-loaded specimens in different Inconel 182 welds, which were exposed to Oskarshamn within a different project (b) [32].

The test results are thus as expected and fit well to lab and service experience with SCC of C & LAS components [4] and dissimilar weld joints [17 – 20, 23 – 48] accumulated during the last decades worldwide (Sections 3.1 and 3.2):

- No or very minor TG SCC has been observed in RPV steels under representative NWC and HWC conditions, and the mean apparent SCC CGRs were rather slow and well below the BWRVIP-60 SCC DL 1 (Figures 22 and 24). Although the extent of cracking in Specimen 402 was rather surprising for a bolt-loaded specimen, the average SCC CGR of 0.5 mm/year over the five-year testing period was still in the upper bound range of constant load SCC CGRs in autoclave tests in oxygenated high-purity water and below the BWRVIP-60 SCC DL 1, and thus does not represent an immediate concern. The initial K_I value of this specimen represents a rather deep crack in the RPV and was close to the K_I range of 50 to 70 $\text{MPa}\cdot\text{m}^{1/2}$, where accelerated SCC is usually observed in high-purity water, in particular in high-sulphur steels.
- ID SCC was observed in the Inconel 182 weld metal under NWC and HWC conditions, but with significantly slower CGRs under HWC conditions (see Figure 25). The apparent SCC CGRs were within the lower range of typical SCC CGRs in Inconel 182 weld metals under NWC and HWC conditions.
- The ID SCC cracks in the specimens with Inconel 182 cladding and fatigue pre-crack tip in the weld metal tested under NWC conditions propagated into the coarse grain peak hardness zone of the LAS HAZ to a limited extent (e.g., Figures 26 and 27). The extent of cracking is not unexpected for an initially growing crack in combination with a possibly increased susceptibility of the peak hardness region in the coarse grain zone, in particular if excessive hardness or martensite-like microstructure is observed. In the interface region of the bi-metallic weld with different thermal expansion coefficients, dynamic straining during thermal transients (e.g., start-up/shut-down) might have contributed or stimulated crack growth in this region. The results also clearly show that cracks may cross the fusion line and enter to the adjacent LAS.
- Secondary cracking (probably due to EAC eventually in connection with local lack of fusion, hot cracking or excessive hardness) in weld metal/RPV HAZ along the fusion line perpendicular to the specimen mid-plane in specimens with Inconel 182 cladding tested under NWC conditions has been observed similar to many other lab investigations [44, 46, 50] (see Figure 28). This indicates a potentially increased EAC susceptibility of this region.



Figure 26: Back scatter electron SEM macrograph of specimen 301, with fatigue pre-crack tip in Inconel 182 weld metal. ID SCC and thumb-nail-shaped crack extension to weld HAZ of RPV steel can be clearly seen [3].

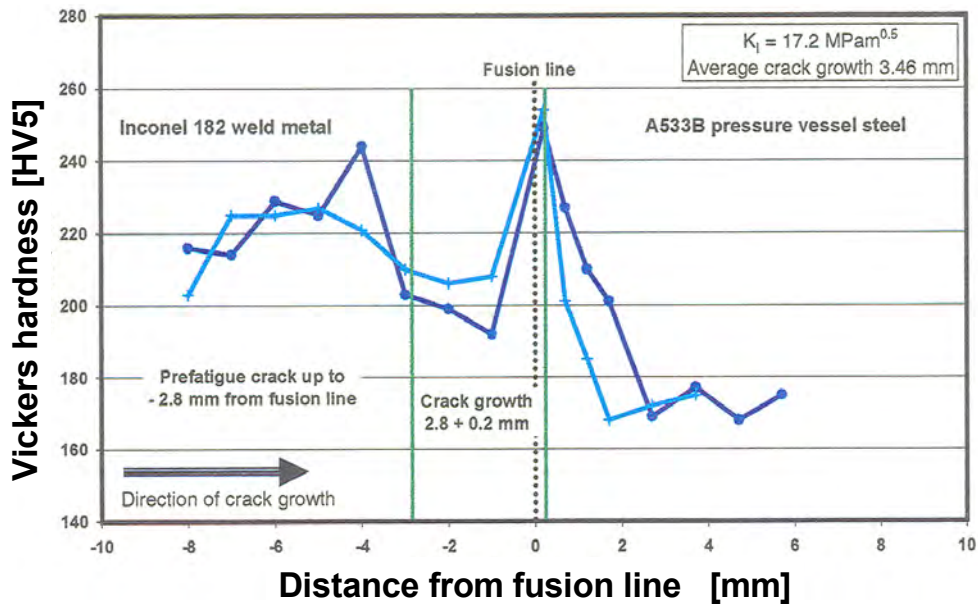


Figure 27: Vickers hardness profile of specimen 301 with location of pre- and final crack-tip and of fusion line showing limited crack extension to peak hardness region of weld HAZ of RPV steel [3].

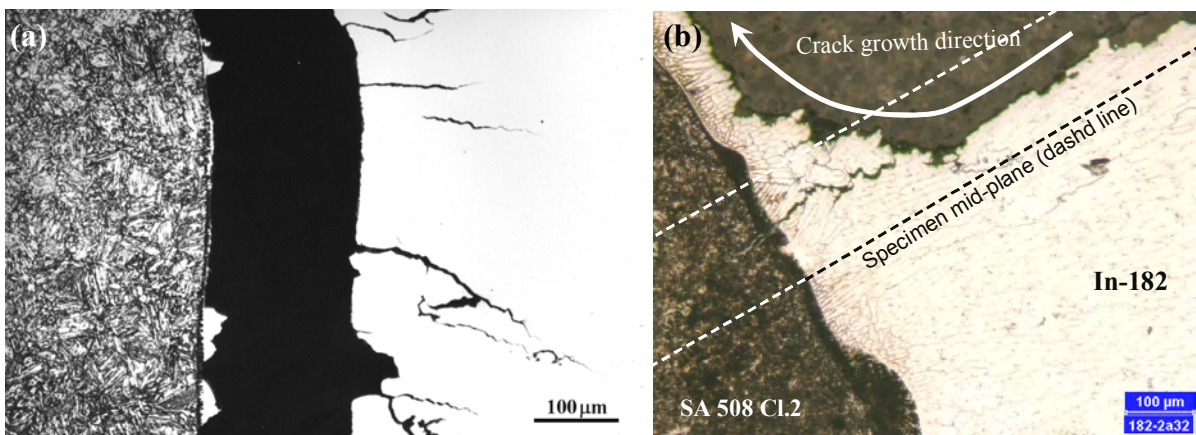


Figure 28: Crack growth in weld metal along the fusion line in Specimen 302 exposed to NWC environment in Oskarshamn 3 (a) and in an Inconel 182-SA 508 Cl.2 weld joint tested under simulated NWC conditions at PSI (b) [56].

The relevant TG SCC crack extension in specimen 402 (Figure 29), which was clad with Inconel 182 and where the fatigue pre-crack tip was located in the unaffected RPV base metal far away from the fusion line (5 to 7.5 mm), was the only surprising result, although the mean apparent SCC CGR was still very slow and below the BWRVIP-60 SCC DL 1 (Figure 22). Specimen 402 is therefore further discussed in the following Section.

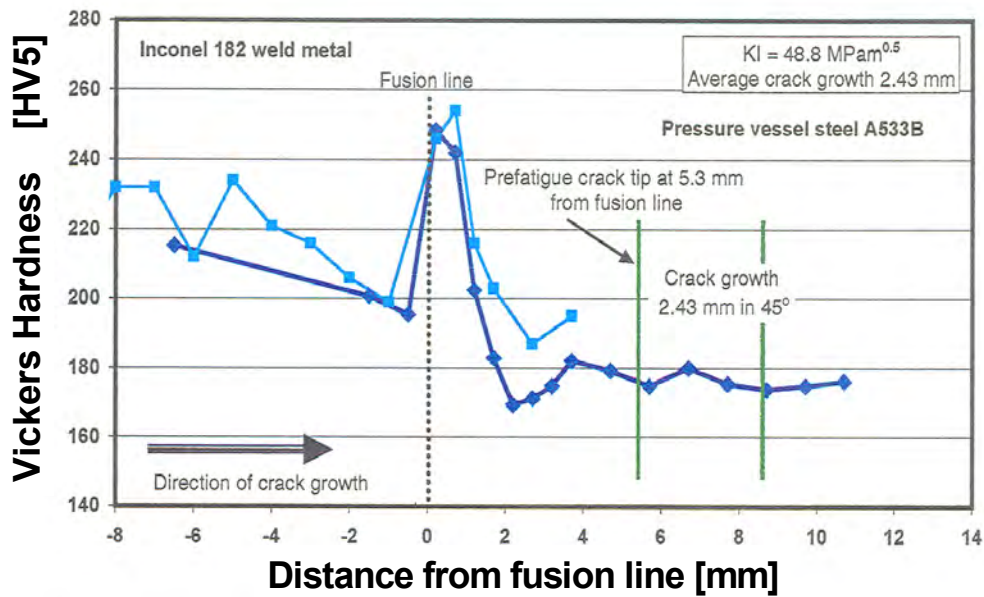


Figure 29: Vickers hardness profile of specimen 402 with location of pre- and final crack-tip and of fusion line showing marked crack extension in RPV base metal [3].

4.3 Assessment and Possible Explanation for SCC in Specimen 402

In the specimens with only minor crack growth in the pressure vessel steel, the crack growth had mainly the appearance of a corroded groove with local TG or IG cracking observed at the tip of the grooves. This may be a result of a very small crack growth in connection to each interruption and start-up of the test. These phases can include a small positive strain rate at the crack-tip, changes in the water chemistry, etc., which can affect crack initiation and growth. This very small crack growth may then have arrested and followed by general corrosion during the test period at normal operation at HT water creating the groove.

In contrast to that, specimen 402 revealed very clear evidence for SCC. Although heavily oxidized during the prolonged exposure periods in NWC water, the fracture surface of specimen 402 revealed the characteristic striationless macro-fractographic appearance of SCC or SICC, i.e., the terrace-like quasi-cleavage structure (Figures 30 and 31). The fracture surface revealed branching, in particular in the middle of the specimen, where the crack has grown out of the mid-plane at an angle of 45° and multiple SCC initiation at different locations and levels (Figures 30 to 32). Many of the individual crack terraces were fan-shaped and the crack front was very uneven. The feather morphology and facets have been destroyed by the oxide film growth even at the final crack front, which thus indicates that the crack was not growing until the end of the exposure in BWR/NWC environment. Nevertheless, the local crack growth direction could be readily recognized and strongly deviated from the macroscopic crack growth direction. All these features are characteristic for SCC under static loading conditions with large crack extensions. Although the high local sulphur content in this specimen was clearly beneficial in stimulating SCC, no direct influence of MnS-inclusions on the fracture morphology was observed.

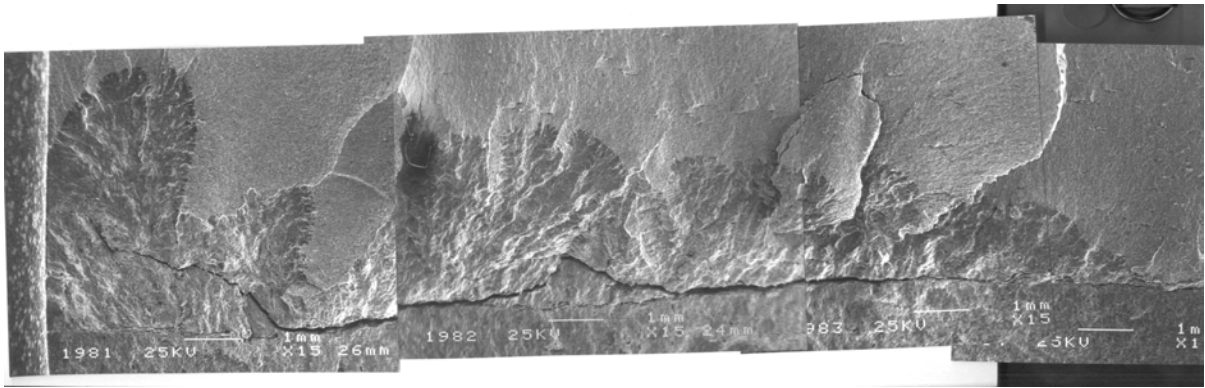


Figure 30: SEM macrograph of Specimen 402 with uneven SCC crack growth through multiple crack initiation and crack branching [3].

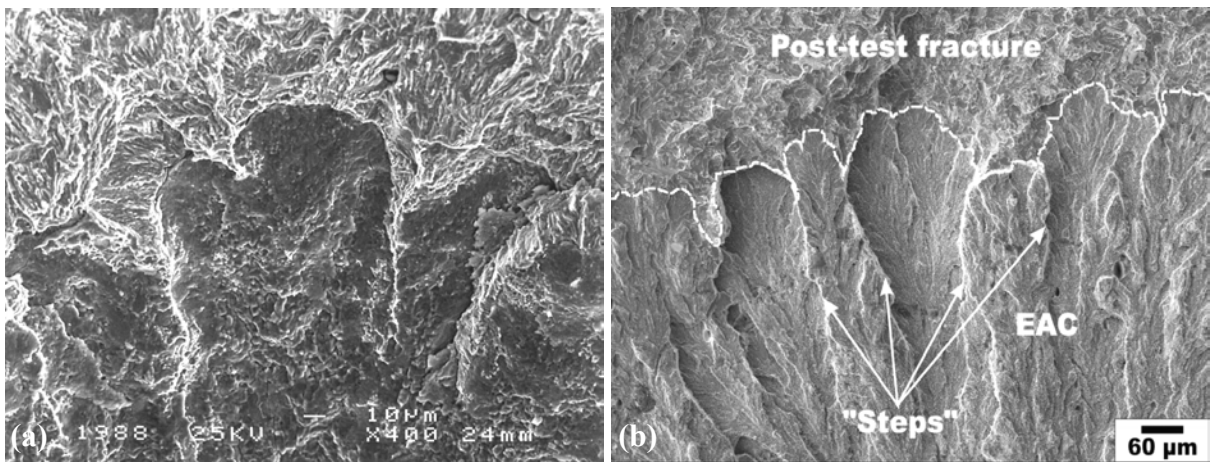


Figure 31: Typical terrace-structure of SCC in specimen 402 (a) and in a specimen from an autoclave test under BWR/NWC conditions at PSI, which showed SCC (b).

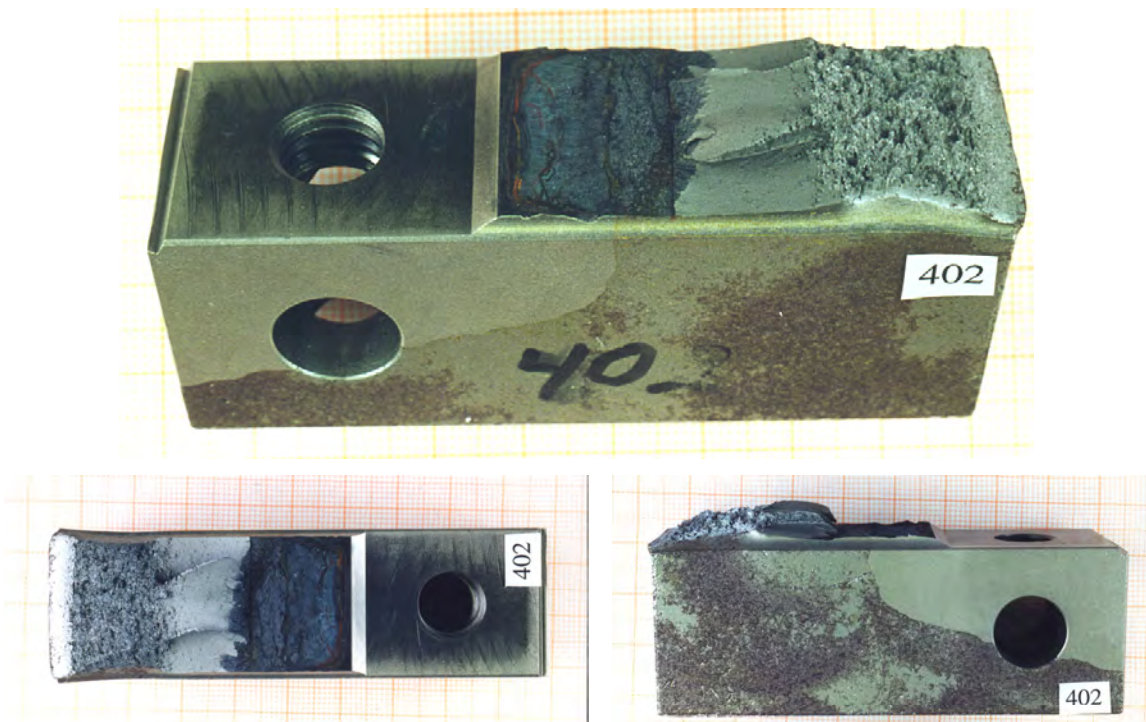


Figure 32: Macrophotos of Specimen 402, which clearly reveal the multiple SCC crack initiation at different levels, crack branching, and uneven crack advance [3].

The microstructural investigations did not reveal any features, which could easily explain the deviation of crack growth in an angle of 45 ° in the middle of the specimen. On the other hand, visual and microhardness examinations revealed no indications for overloading of the specimen. Neither an excessive plastic zone size, nor significant deformation in the crack-tip region at the specimen surface, nor a large crack opening angle were observed. Out-of-mid-plane SCC cracking has sometimes been observed under small scale yielding conditions at PSI, in particular at intermediate temperatures in steels with a high DSA susceptibility [4]. From a mechanic point of view, cracks can easily leave the mid-plane in C(T) specimens, in particular in specimens with a long ligament. Although this results in mixed mode loading, there is still a significant mode-I stress intensity factor K_I working at the crack-tip even for an angle of 90 °.

The detailed post-test fracto- and metallography has thus confirmed, that cracking in this specimen was due to SCC and it could be neither related to any mistreatment of specimen (e.g. , mechanical overloading, too high heat input during welding), welding defects, testing artefacts nor to any microstructural anomalies (e.g., excessive hardness). Therefore, the crack growth in specimen 402 is SCC and represents a valid test results. Specimen 402 has the characteristic fine-grained bainitic microstructure of RPV steels. The increased local sulphur content in this specimen is not an anomaly. Inhomogeneous distribution of MnS and MnS-clustering are quite frequently observed in large LAS plates and forgings. The fatigue pre-crack-tip in specimen 402 is far beyond the fusion line in the unaffected RPV base metal. Therefore, weld residual stress (which were further mitigated by PWHT and specimen cutting) and thermal stress from the different thermal expansion coefficient of the cladding and LAS or the bolt material X-750 do not result in a significant change in K_I and dynamic straining of crack-tip during start-up/shut-down.

Based on recent lab experiments at PSI with chloride addition (Section 3.1.4), an alternate explanation for the cracking in this specimen could be given: The overwhelming part of crack growth might also have occurred during the 20 day chloride transient of 5 to 30 ppb, which happened during the third year of exposure because of a condenser leakage briefly after an outage, where some crack-tip straining or local SCC/SICC crack growth might still have been present (Table 4 and Figure 33). Based on PSI investigations, a SCC CGR of $5 \cdot 10^{-9}$ m/s in the K_I range of $50 \text{ MPa} \cdot \text{m}^{1/2}$ may be expected in oxygenated HT water with a DO of 400 ppb and 10 to 50 ppb of chloride. As shown in Table 4, accelerated SCC during this chloride excursion may easily explain the whole crack extension in specimen 402, and if it is assumed that the whole SCC crack growth occurred during this transient, the apparent SCC CGR fits well to the PSI results (Figure 33). This was further confirmed by the DCPD measurements during the shut-down periods, which indicated that more than 80 % of the crack growth had occurred during the third year of exposure (Figure 34).

	1 day	10 day	1 month
5E-9 m/s	0.43 mm	4.32 mm	12.96 mm
1E-9 m/s	0.09 mm	0.86 mm	2.59 mm

Table 4: Possible SCC crack extension during chloride excursions under simulated BWR/NWC conditions with chloride contents of 10 to 50 ppb, if accelerated SCC crack growth occurs with typical SCC CGRs from PSI investigations in the K_I range of $50 \text{ MPa} \cdot \text{m}^{1/2}$. The average crack advance in specimen 402 was 2.43 mm.

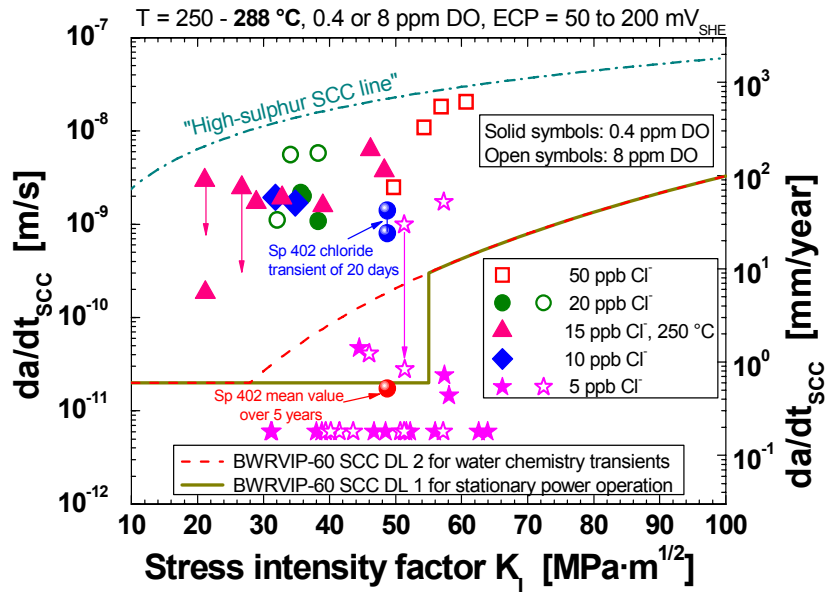


Figure 33: Comparison of apparent SCC CGR of specimen 402 with SCC CGRs from PSI tests with chloride excursions, if it is assumed that SCC had occurred during the condenser leakage during the third year of exposure.

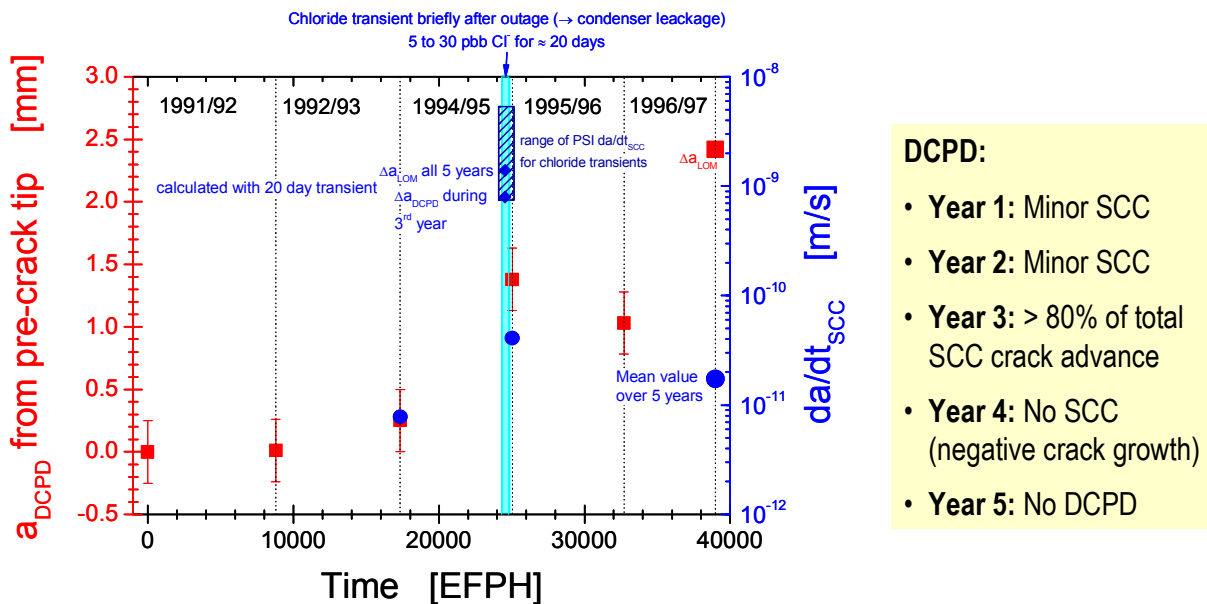


Figure 34: Results from DCPD measurements of Specimen 402 before exposure to BWR/NWC environment in Oskarshamn 3 and during the shut-down periods. The DCPD indicates that the overwhelming part of SCC had occurred during the third year of exposure, when the condenser leakage and chloride excursion happened. The negative crack advance in the subsequent exposure year might be the result of crack arrest and oxide crack bridging and seems also to be confirmed by the heavily corroded fracture surface at the final crack front.

Acceleration of SCC crack growth during a temporary chloride excursion under pure static loading conditions already requires some “active” crack growth before the chloride transient happens, otherwise no acceleration of SCC is observed during short-term transients. Although very slow SCC with local CGRs < 0.6 mm/year (usually restricted to the direct vicinity of MnS-inclusions, which are intersected by the crack front) can occur in C & LAS base metal in high-purity water, it is a rather rare phenomenon at K_I levels < 60 $\text{MPa}\cdot\text{m}^{1/2}$. In case

of non-growing “dormant” cracks, which is more typical for high-purity water and K_I levels $< 60 \text{ MPa}\cdot\text{m}^{1/2}$, an oxide film rupture has to be induced by a load increase or partial un/reloading cycle or any other source of dynamic crack-tip straining during the period where a high chloride concentration still prevails in the crack-tip environment. This is the reason why most specimens tested under NWC did not reveal SCC during the chloride transient. The high local sulphur content and K_I value of specimen 402 have probably favoured some local SCC/SICC crack growth, whereas in most other specimens no EAC occurred and chloride excursion therefore did not result in accelerated SCC crack growth.

5 Summary and Conclusions

The Swedish SCC data from bolt-loaded C(T) specimens of different RPV steels, which have been exposed to BWR/NWC and HWC environment in Oskarshamn 3 and 2 have been critically reviewed and assessed on the basis of the relevant service experience and of the accumulated experimental background knowledge.

The investigations in Oskarshamn 3/2 generally revealed a low SCC crack growth susceptibility of RPV steels and ID SCC in the Inconel 182 weld metal under BWR/NWC and HWC conditions. All non-cladded specimens and specimens with AISI 308L stainless steel cladding revealed no or only minor crack growth under both BWR/NWC and HWC conditions. However, the specimens with Inconel 182 cladding and fatigue pre-crack in the weld metal revealed clear but minor crack growth into the HAZ of the RPV steel under BWR/NWC conditions. Marked crack growth of 2.43 mm in the RPV steel was only observed in one of the Inconel 182 cladded specimens tested under BWR/NWC conditions with a high K_I value of $48.8 \text{ MPa}\cdot\text{m}^{1/2}$, where the fatigue pre-crack-tip was located in the RPV steel base metal far beyond its HAZ. Detailed post-test fracto- and metallography confirmed that cracking in this specimen was due to SCC and it could be neither related to any mistreatment of specimen, welding defects, testing artefacts nor to any microstructural anomalies.

Although the extent of cracking was rather surprising for a bolt-loaded specimen, the average SCC CGR of 0.5 mm/year over the five-year testing period was still within the upper range of constant load SCC CGRs in autoclave tests in oxygenated high-purity water and below the BWRVIP-60 SCC DL 1, and thus does not represent an immediate concern. The initial K_I value of this specimen represents a rather deep crack in the RPV and was close to the K_I range of 50 to $70 \text{ MPa}\cdot\text{m}^{1/2}$, where accelerated SCC is usually observed in high-purity water, in particular in high-sulphur steels. Based on recent lab experiments at PSI with chloride excursions, an alternate explanation for the cracking in this specimen could be given: The overwhelming part of crack growth might also have occurred during a 20 day chloride transient of 5 to 30 ppb, which happened during the third year of exposure because of a condenser leakage briefly after an outage, where some crack-tip straining or local SCC/SICC crack growth might still have been present. This was also further confirmed by the DCPD measurements during the shut-down periods, which indicated that more than 80 % of crack growth had occurred during the third year of exposure.

The test results fit well to the experimental background knowledge and have basically confirmed the excellent service record of properly fabricated C & LAS primary pressure-boundary components and of stainless steel claddings, where no cases of SCC were observed so far. The specimens with the susceptible Inconel 182 cladding and fatigue pre-crack in the weld metal revealed clear, but minor crack growth into the HAZ of the RPV steel under BWR/NWC conditions. They thus confirm the possibility of SCC crack growth through the fusion line into the adjacent RPV steel, although in the field cracking in dissimilar welds was usually confined to the weld metal and some lab experiments revealed cessation of SCC at the fusion boundary. Based on the test data in Oskarshamn 3 and lab experience, the possibility of slow SCC crack growth with CGRs $< 0.6 \text{ mm/year}$ at K_I values $< 60 \text{ MPa}\cdot\text{m}^{1/2}$ in the unaffected RPV base metal cannot be fully excluded. There is thus a certain risk that an ID SCC crack in the Inconel 182 weld metal of an attachment weld or in regions with Inconel 182 cladding might propagate to the adjacent RPV steel. Even in this rare case, only very limited SCC/SICC cracking in RPVs is expected as long as prolonged and severe chloride excursions are avoided and the number of plant transients is limited.

6 Recommendations

Based on the situation described in the previous Sections, it is recommended to perform careful flaw tolerance evaluations (e.g., based on the BWRVIP-60 SCC DLs and the Code Case N-643 EAC curve) for different relevant Inconel 182 weld configurations with initial cracks, which slightly reach into the RPV steel, to estimate the effective margins with respect to current intervals of the periodic in-service inspection. If margins are sufficiently high, no further immediate actions are necessary. The reliable measurement/modelling of the residual stress profiles in such attachment welds may be essential to avoid any undue conservatism in such structural integrity assessments.

Whether or not an ID SCC crack in the weld metal may cross the fusion line and enter into the adjacent RPV steel can strongly depend on the main dendrite orientation (solidification structure), the distribution of grain boundary misorientation in the weld, the plastic weld shrinkage strain and residual stress levels/profiles with respect to the RPV, as well as on the extent of dilution between weld and base metal or possibility of susceptible microstructures/excessive hardness in the weld HAZ, etc. Therefore analysis of weld metallurgy/residual stress profiles of relevant Inconel 182 attachment welds and claddings could help to identify regions with the highest risk.

If further reactor site testing is considered, the authors would place the focus on tests under BWR/NWC conditions with Inconel 182-RPV weld joints (which are representative for relevant Swedish configurations) with fatigue pre-crack-tips close to the fusion line and realistic initial K_I values to study the crack extension to the RPV over prolonged periods. Tests with specimens with crack planes parallel to the fusion boundary or weld configurations with more favourable dendrite orientations or Inconel 82 weldments could complete the testing programme. If possible, some specimens should also be tested in lab experiments under comparable environmental conditions and active external load with continuous online crack length measurements by DCPD.

Although there is no direct evidence from the field, with respect to SCC risks in RPVs, the effect of chloride excursions on SCC crack growth in RPV steels under BWR/NWC conditions, and in particular the possibility of long-term effects after severe and prolonged transients, should be further evaluated in lab experiments. Long-term tests with bolt-loaded specimens and moderate chloride contents of 5 to 20 ppb could complete such a testing programme. Studies on the possible interaction between chloride and oxide films/repassivation in HT water could help to better understand the effect of chloride on the SCC behaviour.

7 Acknowledgements

This report was sponsored by the Swedish Nuclear Safety Inspectorate SKI, which is gratefully acknowledged. The evaluation of the Swedish data is mainly based on the insights, which have been gained by the authors over the last decade within several PSI research projects (SpRK-I: 1996 – 1999, RIKORR-I: 2000 – 2002, RIKORR-II: 2002 – 2005, CASTOC-EU5: 2000 – 2003), which were sponsored by the Swiss Federal Nuclear Safety Inspectorate (HSK), the Swiss Federal Office of Energy (BFE), the Swiss Federal Office for Education and Science (BBW), and the Swiss utilities (Swissnuclear). The results on SCC crack growth in the interface region of the Inconel 182-SA 508 Cl.2 weld joint are from a small collaboration between the Fracture Research Institute (FRI) of the Tohoku University and PSI, which is part of the PEACE-II/III (sponsored by EDF, SKI, EPRI, TEPCO, KEPCO, Tohoku EPCO, JAPCO, Hitachi, Toshiba, and MHI) and RIKORR-II/KORA project. The authors are also grateful to Ulla Ehrnstén from VTT for providing SEM micrographs for this report.

8 References

- [1] **M.O. SPEIDEL, R.M. MAGDOWSKI**, *International Journal of Pressure Vessel & Piping*, **34**, pp. 119 – 142, 1988.
- [2] **I. BENGTTSSON, J. ERIKSSON**, "Final Report on Reactor Pressure Vessel Steel Testing in Oskarshamn 2 and Okarshamn 3", ABB Atom Report SBR 99-020, November 1999.
- [3] **U. EHRNSTÉN**, "Fractographic and Metallographic Investigations on Pressure Vessel Steel C(T) Specimens Tested in BWR Environment", VTT Research Report VAL62-001675, VTT, Espoo, Finland, September 2000.
- [4] **H.P. Seifert, S. Ritter**, "Research and Service Experience with Environmentally-Assisted Cracking in Carbon and Low-Alloy Steels in High-Temperature Water", SKI Report, SKI, Stockholm, Sweden, 2005 (to appear).
- [5] **E.F. WALKER, M.J. MAY**, B.I.S.R.A. Report MG/E/307/67, 1967.
- [6] **A. KRAUS**, "Stress Corrosion Cracking of Pressure Vessel Steels in High-Temperature Water", Ph.D. thesis, Diss. ETH Nr. 10644, ETH Zürich, 1994.
- [7] **J. HELDT, H.P. SEIFERT**, *Nuclear Engineering & Design*, **206**, pp. 57 – 89, 2001.
- [8] **J. FÖHL, T. WEISENBERG**, "Corrosion Assisted Crack growth in Base Material of High and Low Strength Ferritic Steel under Static Load with and without Intermediate Unloadings in Oxygen Containing High Temperature Water of Different Conductivity", Final Report Reactor Safety Research-Project No. 150 1229, Technical Report, MPA-Auftragsnummer 8874 00 0001, MPA Stuttgart, Stuttgart, Germany, October 2004.
- [9] **H.P. SEIFERT, S. RITTER**, "New Observations About the SCC Crack Growth Behaviour of Low-Alloy RPV Steels Under BWR/NWC Conditions", Proc. 11th Int. Conf. on Environmental Degradation of Materials in Nuclear Power Systems – Water Reactors, CD-ROM, NACE/TMS/ANS, Stevenson, WA, USA, August 10 – 14, 2003.
- [10] **B. CHENG et al.**, "BWR Water Chemistry Guidelines – 1996 Revision", EPRI Report TR-103515-R1, Palo Alto, December 1996.
- [11] **M. LASCH, U. STAUDT**, *VGB-Kraftwerkstechnik*, **75**, pp. 745 – 750, 1995.
- [12] Personal communication with **B. AGHILI (SKI)**.
- [13] **A. ROTH et al.**, "The Effect of Transients on the Crack growth Behaviour of Low Alloy Steels for Pressure Boundary Components under Light Water reactor Conditions", Proc. 12th Int. Conf. on Environmental Degradation of Materials in Nuclear Power Systems – Water Reactors, CD-ROM, NACE/TMS/ANS, Snowbird, Utah, USA, August 14 – 18, 2005.
- [14] **S. RITTER, H.P. SEIFERT**, *Power Plant Chemistry*, **6**, pp. 748 – 760, 2004.
- [15] **S. RITTER, H.P. SEIFERT**, "The Effect of Chloride and Sulfate Transients on the Stress Corrosion Cracking Behaviour of Low-Alloy RPV Steels Under Simulated BWR Environment", NACE Corrosion 2004, CD-ROM, Paper No. 04680, NACE, New Orleans, LA, USA, March 28 – April 1, 2004.
- [16] **H.P. Seifert, S. Ritter**, *Chimia*, **59**, 2005 (to appear).
- [17] **R.M. HORN, P. L. ANDRESEN, J. HICKLING**, "BWR Alloy 182 Stress Corrosion Cracking Experience", 5th Int. Symp. on Contribution of Materials Investigation to the Resolution of Problems Encountered in Pressurized Water Reactors (Fontevraud 5), CD-ROM, Fontevraud, France, September 23 – 27, 2002.

- [18] **R. S. PATHANIA, A. R. MCILREE, J. JICKLING**, "Overview of Primary Water Cracking of Alloys 182/82 in PWRs", 5th Int. Symp. on Contribution of Materials Investigation to the Resolution of Problems Encountered in Pressurized Water Reactors (Fontevraud 5), CD-ROM, Fontevraud, France, September 23 – 27, 2002.
- [19] **P.L. ANDRESEN, L.M. YOUNG, P.W. EMIGH, R.M. HORN**, "Stress Corrosion Crack Growth Rate Behavior of Ni Alloys 182 and 600 in High Temperature Water", NACE Corrosion 2002, CD-ROM, Paper No. 02510, NACE, 2003.
- [20] **R. LINDSTRÖM, P. LIDAR, J. LAGERSTRÖM**, "Crack Growth of Alloy 182 in a Simulated Primary Side PWR Environment", Proc. 8th Int. Conf. on Environmental Degradation of Materials in Nuclear Power Systems – Water Reactors, Vol. 1, pp. 422 – 429, ANS/TMS/NACE, Amelia Island, Florida, USA, August 10 – 14, 1999.
- [21] **T. MATSUNAGA, K. MATSUNAGA**, "Stress Corrosion Cracking of CRD Stub Tube Joint and Repair at Hamaoka Unit 1", Proc. 11th International Conference on Nuclear Engineering, Paper ICONE11-36056, Shinjuku, Tokyo, Japan, April 20 – 23, 2003.
- [22] **A. YAMASHITA, K. TAKEUCHI, W. SAGAWA, F. MANABE**, "The Stress Corrosion Cracking at Shroud Support Tsuruga Unit 1", Proc. 9th International Conference on Nuclear Engineering, Paper ICONE 9- 66, April 8-12, 2001, Nice, France.
- [23] **E.A. WIMUNC**, *Power Reactor Technology*, **9**, pp. 101 – 109, 1966.
- [24] **T. KONODEO et al.**, *Nuclear Engineering & Design*, **16**, pp. 205 – 222, 1971.
- [25] **A.J. GIANNUZZI**, "Evaluation of reactor Pressure Vessel Head cracking in Two Domestic BWRs", EPRI Final Report TR-101971, February 1993.
- [26] **B.M. GORDON et al.**, *ASM PVP*, **119**, pp. 9 – 17, 1987.
- [27] **M. ITOW, M. KIKUCHI, N. ZANAKA**, "The Influence of Corrosion Potential on SCC Growth Behaviour of a Deep Crack in Alloy 182 in Simulated BWR Environment", Proc. 11th Int. Conf. on Environmental Degradation of Materials in Nuclear Power Systems – Water Reactors, 2003, CD-ROM, ANS/TMS/NACE, Skamania Lodge, Stevenson, WA, USA, August 10 – 14, 2003.
- [28] **A. TOIVONEN, P. AALTONEN, L. TAIVALAHO, P. MOILANEN, E. MUTTILAINEN**, "Effects of Water Chemistry Transients on Crack Growth Rate of Nickel-Based Weld Metals", Proc. 10th Int. Conf. on Environmental Degradation of Materials in Nuclear Power Systems – Water Reactors, 2001, CD-ROM, ANS/TMS/NACE, Lake Tahoe, Nevada, USA, August 5 – 9, 2001.
- [29] **O.K. CHOPRA, W.K. SOPPET, W.J. SHACK**, "Effects of Alloy Chemistry, Cold Work, and Water Chemistry on Corrosion Fatigue and Stress Corrosion Cracking of Nickel Alloys and Welds", NURE/CR-6721, NRC, April 2001.
- [30] **M. ITOW, Y. ABE, H. SAKAMOTO, S. HIDA, K. TAKAMORI, S. SUZUKI**, "The Effect of Corrosion Potential on Alloy 182 Crack Growth Rate in High Temperature Water", Proc. 8th Int. Conf. on Environmental Degradation of Materials in Nuclear Power Systems – Water Reactors, Vol. 2, pp. 712 - 719, ANS, Melia Island, Florida, USA, August 10 – 14, 1999.
- [31] **A. JENSEN, M. STIGENBERG, L.G. LJUNGBERG**, "Initiation of Stress Corrosion Cracking in Alloys 600 and 182", Proc. 9th Int. Conf. on Env. Deg. of Mat. in Nucl. Power Systems – Water Reactors, pp. 331 – 337, Newport Beach, CA, USA, August 1 – 5, 1999.

- [32] **L. G. LJUNGBERG, M. STIGENBERG**, "Stress Corrosion Cracking Propagation in Low-Strength Nickel-Base Alloys in Simulated BWR Environment", Proc. 8th Int. Conf. on Environmental Degradation of Materials in Nuclear Power Systems – Water Reactors, Vol. 2, pp. 704 – 711, ANS, Melia Island, Florida, USA, August 10 – 14, 1999.
- [33] **U. MORIN, C. JANSSON, B. BENGTSON**, "Crack Growth Rates for Ni-Base Alloys with the Application to an Operating BWR", Proc. 6th Int. Conf. on Environmental Degradation of Materials in Nuclear Power Systems – Water Reactors, pp. 373 – 377, TMS, San Diego, California, August 1 – 5, 1993.
- [34] **L. G. LJUNGBERG, P. STAHL, J. L. NELSON**, "Stress Corrosion Cracking Initiation in Alloys 600 and 182", Proc. 6th Int. Conf. on Environmental Degradation of Materials in Nuclear Power Systems – Water Reactors, pp. 379 – 384, TMS, San Diego, California, August 1 – 5, 1993.
- [35] **G. Nakayama, M. Akashi**, "Effect of Electrode Potential on the Susceptibility of Alloy 182 Weld Metal to Stress-Corrosion Cracking in Simulated BWR Environment", Proc. 6th Int. Conf. on Environmental Degradation of Materials in Nuclear Power Systems – Water Reactors, pp. 883 – 887, TMS, San Diego, California, August 1 – 5, 1993.
- [36] **P. L. ANDRESEN**, *Corrosion*, **47**, pp. 917 – 938, 1991
- [37] **P. ANDRESEN**, *Corrosion Science*, **44**, pp. 376 – 385, 1988.
- [38] **A. MCMINN, R. A. PAGE**, *Corrosion*, **44**, pp. 239 – 247, 1988.
- [39] **P. ANDRESEN**, "Effects of Dissolved Oxygen, Solution Conductivity and Stress Intensity on the Interdendritic Stress Corrosion Cracking of Alloy 182 Weld Metal", NACE Corrosion 87, Paper No 85, March 9-13, 1987, Moscone Center, San Francisco, California.
- [40] **R.A. Page**, *Corrosion*, **39**, pp. 409 – 421, 1983.
- [41] **W. H. BAMFORD, J. P. FOSTER, AND R. S. PATHANIA**, "An Investigation of Alloy 182 Stress Corrosion Cracking in Simulated PWR Environment", Proc. 9th International Symposium on Environmental Degradation of Materials in Nuclear Power Systems – Water Reactors, pp. 279 - 295, NACE/TMS/ANS, Newport Beach, USA, August 1 – 5, 1999.
- [42] **T. CASSAGNE et al.**, "Stress Corrosion Crack Growth Rate Measurements in Alloys 600 and 182 in Primary Water Loops under Constant Load", Proc. 9th International Symposium on Environmental Degradation of Materials in Nuclear Power Systems – Water Reactors, pp. 217 – 224, NACE/TMS/ANS, Newport Beach, USA, August 1 – 5, 1999.
- [43] **S. L. HONG et al.**, "Measurements of Stress Corrosion Cracking Growth Rates in Weld Alloy 182 in Primary Water of PWR", Proc. of 10th Int. Conf. on Environmental Degradation of Materials in Nuclear Power Systems – Water Reactors, NACE/TMS/ANS, CD-ROM, Lake Tahoe, Nevada, USA, August 6 – 10, 2001.
- [44] **D. R. TICE, W. DIETZEL, A. TOIVONEN, D. I. SWAN, B. ROSBORG, J. LAPENA, J.D. ATKINSON, S. MCALLISTER**, "Evaluation of Test techniques for Stress Corrosion Cracking of Dissimilar Weldments", Proc. 10th Int. Conf. on Environmental Degradation of Materials in Nuclear Power Systems – Water Reactors, 2001, CD-ROM, ANS/TMS/NACE, Lake Tahoe, Nevada, USA, August 5 – 9, 2001.
- [45] **G.F. LI, J. CONGLETON**, *Corrosion Science*, **42**, pp. 1005 – 1021, 2000.

- [46] **P. HURST, A. S. RAFFEL, D. R. TICE**, "Environmental Degradation of Dissimilar Metal Welds", Proc. 8th Int. Conf. on Environmental Degradation of Materials in Nuclear Power Systems – Water Reactors, Vol. 1, pp. 430 – 438, ANS, Melia Island, Florida, USA, August 10 – 14, 1999.
- [47] **M. RUSCAK et al.**, *International Journal of Pressure Vessel & Piping*, **68**, pp. 23 – 37, 1996.
- [48] **R. Page**, *Corrosion*, **41**, pp. 338 – 344, 1985.
- [46] **Q. PENG, H. YAMAUCHI, T. SHOJI**, "Dendrite Boundary Microchemistry in Alloy 182 Weld Metal", Proc. 11th Int. Conf. on Environmental Degradation of Materials in Nuclear Power Systems – Water Reactors, 2003, CD-ROM, ANS/TMS/NACE, Skamania Lodge, Stevenson, WA, USA, August 10 – 14, 2003.
- [49] **Q. J. Peng et al.**, *Metall. Mater. Trans. A*, **34A**, pp. 1891 – 1899, 2003.
- [50] **Q. PENG, T. SHOJI, S. RITTER, H.P. SEIFERT**, "SCC Behaviour in the Transition Region of an Alloy 182-SA 508 Cl.2 Dissimilar Weld Joint under Simulated BWR/NWC Conditions", Proc. 12th Int. Conf. on Environmental Degradation of Materials in Nuclear Power Systems – Water Reactors, CD-ROM, NACE/TMS/ANS, Snowbird, Utah, USA, August 14 – 18, 2005.
- [51] Personal communication with **C. JANSSON (SwedPower AB)**.
- [52] **G. SUND**, "Quantifying Manganese Sulphide Inclusions in Pressure Vessel Steels", SKI Report 94:23, SKI, Stockholm, Sweden, 1994.
- [53] **P. ANDRESEN, MM. MORRA, R.M. HORN**, "Effects of Positive and Negative dK/da on SCC Growth Rates", Proc. 12th Int. Conf. on Environmental Degradation of Materials in Nuclear Power Systems – Water Reactors, CD-ROM, NACE/TMS/ANS, Snowbird, Utah, USA, August 14 – 18, 2005.
- [54] **P. ANDRESEN**, "Modelling of Water and Material Chemistry Effect on Crack-Tip Chemistry and Resulting Crack Growth Kinetics", Proc. 3rd Int. Symp. on Environmental Degradation of Materials in Nuclear Power Systems – Water Reactors, TMS-AIME, pp. 301 – 312, 1988.
- [55] **P.L. ANDRESEN**, "Modelling the Effect of Sulphur on the Threshold Environmental Cracking Rate of Steels in High Temperature Water", Proc. 3rd Int. Conf. on Fatigue and Fatigue Thresholds, Midlands, UK, pp. 1189 – 1200, 1987.
- [56] **H.P. SEIFERT, Q. PENG, S. RITTER, T. SHOJI**, "EAC Crack Growth Behaviour in the Transition Region of an Alloy182/SA 508 Cl.2 Dissimilar Weld Joint under Simulated BWR/NWC Conditions", Minutes of the 2005 Annual Meeting of the International Co-operative Group on Environmentally-Assisted Cracking of Water Reactor Materials, CD-ROM, Ed.: J. Hickling, Low Alloy Steel Session, Paper LAS-7, Antwerp, Belgium, April 10 – 15, 2005.

www.ski.se

STATENS KÄRNKRAFTINSPEKTION
Swedish Nuclear Power Inspectorate

POST/POSTAL ADDRESS SE-106 58 Stockholm

BESÖK/OFFICE Klarabergsviadukten 90

TELEFON/TELEPHONE +46 (0)8 698 84 00

TELEFAX +46 (0)8 661 90 86

E-POST/E-MAIL ski@ski.se

WEBBPLATS/WEB SITE www.ski.se